Journal of Photochemistry and Photobiology C: Photochemistry Reviews 24 (2015) 1–15

Contents lists available at ScienceDirect

Journal of Photochemistry and Photobiology C: Photochemistry Reviews

journal homepage: www.elsevier.com/locate/jphotochemrev

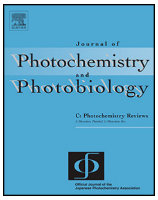

Review

Primary reactions in the photochemistry of hexahalide complexes of platinum group metals: A minireview

Evgeni M. Glebov[a,b,*], Ivan P. Pozdnyakov[a,b], Victor F. Plyusnin[a,b], Igor Khmelinskii[c]

[a] *Voevodsky Institute of Chemical Kinetics and Combustion of SB RAS, 630090 Novosibirsk, Russia*
[b] *Novosibirsk State University, 630090 Novosibirsk, Russia*
[c] *Universidade do Algarve, FCT, DQF and CIQA, 8005-139 Faro, Portugal*

ARTICLE INFO

Article history:
Received 4 June 2014
Received in revised form 7 May 2015
Accepted 11 May 2015
Available online 15 May 2015

Keywords:
Hexahalide complexes of platinum group metals
Photophysics
Ultrafast pump–probe spectroscopy
Primary processes

ABSTRACT

We review the results obtained for $Pt^{IV}Cl_6^{2-}$, $Pt^{IV}Br_6^{2-}$, $Ir^{IV}Cl_6^{2-}$, $Ir^{IV}Br_6^{2-}$, and $Os^{IV}Br_6^{2-}$ complexes in aqueous and alcoholic solutions using ultrafast pump–probe spectroscopy, laser flash photolysis, ESR, and photoelectron spectroscopy. We discuss the correlations between the photophysics and the photochemistry of these complexes. The key reaction for $Pt^{IV}Cl_6^{2-}$ is the inner-sphere electron transfer, which results in an Adamson radical pair that lives for several picoseconds, and the subsequent photoaquation in aqueous solutions and photoreduction in alcohols. The chlorine atom formed as the primary product escapes the solvent cage in aqueous solutions or oxidizes a solvent alcohol molecule via secondary electron transfer, producing secondary intermediates that react on the microsecond time scale. The photoexcitation of $Pt^{IV}Br_6^{2-}$ results in the formation of pentacoordinated Pt^{IV} intermediates, i.e. $^3Pt^{IV}Br_5^-$ and $^1Pt^{IV}Br_5^-$, with characteristic lifetimes of approximately 1 and 10 ps, respectively. Subsequent reactions of these intermediates result in the complexation of a solvent molecule. Photoreduction is also possible in alcohols. Similar reactions occur with rather low quantum yields for $Ir^{IV}Cl_6^{2-}$, therefore, only the ground-state recovery could be monitored in ultrafast experiments, which occur on the 10-ps time scale. The photochemical behaviours of the $Ir^{IV}Br_6^{2-}$ and $Os^{IV}Br_6^{2-}$ complexes are similar to those of $Ir^{IV}Cl_6^{2-}$ and $Pt^{IV}Br_6^{2-}$, respectively.

Contents

---

[*] Corresponding author. Tel.: +7 383 3332385.
E-mail address: glebov@kinetics.nsc.ru (E.M. Glebov).

http://dx.doi.org/10.1016/j.jphotochemrev.2015.05.003

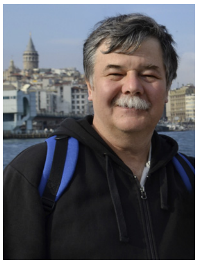

Evgeni M. Glebov received a PhD in Chemical Physics from the V.V. Voevodsky Institute of Chemical Kinetics and Combustion (ICK&C) of the Siberian Branch of the Russian Academy of Sciences (Novosibirsk, Russia) in 1998. His doctoral thesis was supervised by Prof. V. Plyusnin (Novosibirsk). Since 2003, he is a senior researcher in the Laboratory of Photochemistry of ICK&C. His research interests include photophysics and photochemistry of coordination and organic compounds, photochromism, and ecological photochemistry. He is a professor of physics in Novosibirsk State University.

Ivan Pozdnyakov received his master degree in Chemistry from Novosibirsk State University (2001). Subsequently he entered the Laboratory of Photochemsitry of Insitute of Chemical Kinetics and Combustion (ICK&C) of the Siberian Branch of the Russian Academy of Sciences (Novosibirsk, Russia) for the study of environmental photochemistry under supervision of Prof. V. Plyusnin. PhD degree in Physical Chemistry was obtained in 2005. Since 2009 he is a senior researcher of ICK&C. His current research is focused on the investigation of mechanisms and kinetics of photochemical degradation of ecotoxicants in water solutions in presence of environmentally relevant species such as iron complexes and humic substances. His works were awarded twice by Voevodsky's Prize of Siberian Branch of Russian Academy of Science for Young Scientists (2002, 2008). I. Pozdnyakov is an author of more than 45 papers in photochemistry.

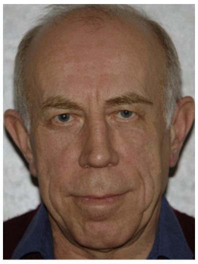

Victor Plyusnin was born in 1946. He graduated the Novosibirsk State University in Physics, specialized in Chemical Physics (1968), and got his candidate degree from the Institute of Chemical Kinetics and Combustion (ICK&C), Novosibirsk, in 1974, doctoral degree in 1992 and became professor in 1993. His doctoral thesis was devoted to the photochemistry of halide complexes of transition metals. His research interests are related to the photochemistry and spectroscopy of different photochemically active, photochromic and light emitting molecular systems. He published over 180 papers in peer-reviewed specialized journals both as an author and coauthor. His interests include education and he published about 10 books/book chapters as professor of physical chemistry department in Novosibirsk State University.

Igor Khmelinskii was born in 1957 in the USSR. He graduated the Novosibirsk State University in Physics, specialized in Chemical Physics (1979), and got his doctoral degree from the Institute of Chemical Kinetics and Combustion (ICK&C), Novosibirsk (1988), and aggregation from the University of Algarve (UAlg), Faro, Portugal (2003). His doctoral thesis was supervised by Prof. V. Plyusnin (Novosibirsk), and post-doctoral work by Prof. F. Wilkinson (Loughborough) and Prof. L. F. Vieira Ferreira (Lisbon). He was affiliated to ICK&C in 1979–1992 as a researcher, and since 1993 to UAlg as an Assistant Professor (presently with Aggregation). Mr. Khmelinskii published over 150 papers in peer-reviewed specialized journals, and several books/book chapters, both as an author and an editor. His interests include education and climate-related issues: http://goo.gl/7yvA7.

1. Introduction

The photochemical activity of platinum group metal complexes was discovered almost 200 years ago [1]. The photochemistry of hexahalide complexes of platinum group metals ($M^{IV}X_6{}^{2-}$) was considered to be a subject of solely academic relevance until the end of the 20th century [2–5]. The principal focus has been on the $Pt^{IV}Cl_6{}^{2-}$ complex. The main points investigated were the reaction intermediates [6–12], unusual aquation chain reactions [11,12] and the dramatic differences in the properties of the isoelectronic $Pt^{IV}Cl_6{}^{2-}$ and $Pt^{IV}Br_6{}^{2-}$ complexes [2,3].

Currently, the practical needs of various technological applications provided new stimuli for photochemical studies of these complexes. The best-known application is in photocatalysis. The four-electron photoreduction of Pt^{IV} to Pt^0 in water–alcohol mixtures discovered by Cameron and Bocarsly [13,14] initiated the use of $Pt^{IV}Cl_6{}^{2-}$ photolysis to produce platinum nanoparticles [15–22]. Generally, the direct photoreduction of metal cations has been established as an important method to produce nanoparticles that are free from chemical reducing agents (see [15] and references therein).

One of the fundamental problem in photocatalysis is extending the absorption spectra of cheap semiconductors (TiO_2, CdS) into the visible spectral range. One excellent approach is modifying TiO_2 [23–27] or CdS [28–30] surfaces with metallic platinum via the photoreduction of hexachloroplatinate. The photochemical modification of the TiO_2 surface by iridium was also reported [31]. Proper descriptions of such systems require knowledge about both the heterogeneous chemistry and photochemistry of the complexes formed by the desorbed metal atoms in solution [24].

Photodynamic therapy (PDT) is another important application of these complexes, joining the high cytotoxicity of platinum group metals to other advantages of PDT, i.e. the selectivity and the low systemic toxicity [32,33]. Typically, platinum complexes are used in PDT, see [32–35] and the references therein. Additionally, the photolysis products of ammonium hexachloroiridate(IV) have been reported to have anti-tumour and antimutagenic activities by Gale et al. [36]. Organoiridium [37] and cyclometallated iridium complexes [33,38,39] were also proposed as prospective anticancer agents.

An interesting application of hexachloroiridates was proposed by Gupta et al. [40,41]. They offered a combined photoelectrochemical method of hydrogen and chlorine production from hydrochloric acid that is assisted by a mixture of $Ir^{IV}Cl_6{}^{2-}$ and $Ir^{III}Cl_6{}^{3-}$ complexes as a photocatalyst.

Successful application of photochemical reactions requires detailed knowledge of the reaction mechanism. A straightforward way to obtain such knowledge is to follow the entire reaction path from the ultrafast primary processes to the final products. In practice, the reaction mechanisms in the photochemistry of coordination compounds were usually proposed based on the results of steady-state experiments because the ability to follow the primary reactions was lacking [2–5]. Often, the involvement of short-living reactive intermediates, such as Adamson's radical pairs [42], has been merely postulated without any direct evidence. Currently, these mechanisms may be examined via advanced time-resolved methods, starting at the femtosecond time resolution.

The study of the ultrafast dynamics of transition metal complexes is an active area of research in chemical physics [43–51]. Nevertheless, primary photophysical processes are known in detail for only a few types of transition metal complexes. These include Cr(III) complexes [46–48], polypyridyl complexes of Ru(II) [43,44,52], and metal carbonyls [43,51]. Additionally, complexes demonstrating spin crossover are being actively studied [50,53].

Presently, we review the experimental work on the primary photophysical and photochemical reactions of $M^{IV}X_6{}^{2-}$ complexes via ultrafast kinetic spectroscopy.

2. Experimental setups, kinetic curves and data treatment

The experiments in the ultrafast kinetic spectroscopy of the $Pt^{IV}Cl_6{}^{2-}$, $Pt^{IV}Br_6{}^{2-}$ and $Ir^{IV}Cl_6{}^{2-}$ complexes were performed using

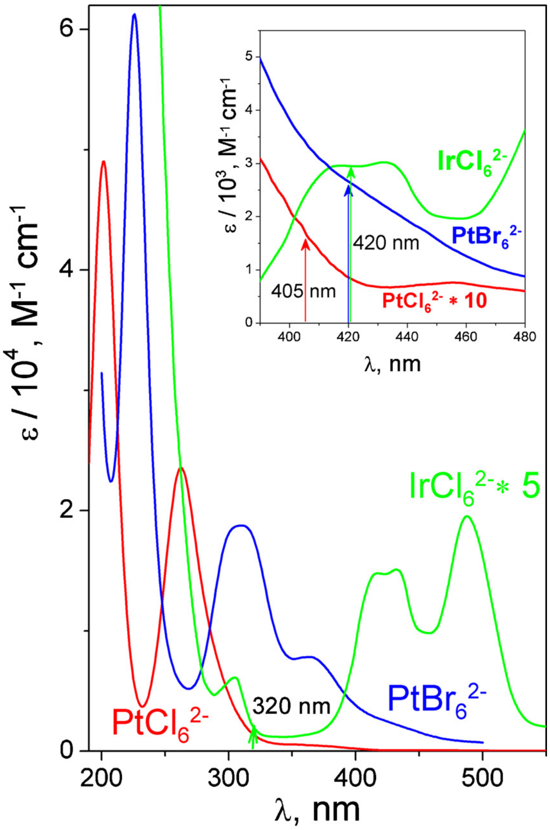

Fig. 1. UV absorption spectra of the $Pt^{IV}Br_6^{2-}$, $Pt^{IV}Cl_6^{2-}$ and $Ir^{IV}Cl_6^{2-}$ complexes in aqueous solutions. The inset shows the visible part of the spectra. The marked excitation wavelengths were used in the ultrafast kinetic measurements.

the experimental setup described in detail earlier [54]. The samples were excited by ~60 fs pulses at 400–420 nm (second harmonic of a Ti:sapphire generator–amplifier system, CDP Ltd., Moscow, Russia, approximately 20–25 μJ/pulse). The excitation pulse repetition rate was 10 Hz, and 200 pulses were needed to record one entire time-resolved spectrum. The samples were placed in a 1-mm rotating cell, to provide uniform irradiation and avoid unwanted thermal effects from heating by the pump pulse. Typically, time-resolved spectra were collected with a delay step of 100 fs during the first 3 ps after excitation (30 time points), and exponentially increasing delay times were used at longer delays. Usually, 60–70 spectra were collected for each sample with the longest delay of approximately 100 ps. The experimental data were fitted globally, typically using a three-exponential model. The fitting programme was corrected for the group velocity dispersion and the calculated response time of the instrument. The global time delay was one of the fitted parameters, defining the arrival of the excitation pulse (time zero). The uncertainty in the time zero was close to 100 fs, which is similar to the delay step, while the overall time resolution was 150–200 fs, determined by the convolution of the pump (excitation) and probe pulses.

An ultrafast pump–probe spectroscopy setup with the UV excitation described in detail in [55] was used in several experiments on $Ir^{IV}Cl_6^{2-}$. The samples were excited by approximately 100 fs pulses at ~320 nm (fourth harmonic of the signal wave of a TOPAS optical parametric amplifier). The excitation energy was approximately 1 μJ/pulse, the excitation pulse repetition rate was 1 kHz, with 200 pulses required to record one complete time-resolved spectrum. The sample solutions (10 ml total volume) were pumped through a 1-mm cell at room temperature, to provide uniform irradiation and avoid possible photodegradation. The experimental data were fitted globally, using two- or three-exponential models. The fitting programme corrected for the group velocity dispersion and calculated the response time of the instrument.

Experiments on ultrafast kinetic spectroscopy of the $Pt^{IV}Br_6^{2-}$, $Ir^{IV}Br_6^{2-}$ and $Os^{IV}Br_6^{2-}$ complexes were performed using the setup described in [56–58]. Two TOPAS-C optical parametric amplifiers generated 420 or 530 nm pump pulses of 2 μJ and probe pulses tunable between 270 and 400 nm. The overall time resolution was 150 fs. High values of the signal-to-noise ratio allowed resolving of the coherent oscillations in the kinetic curves [57,58].

Typically, the kinetic curves obtained in ultrafast pump–probe experiments are fitted globally, using either a biexponential function (1) or a triexponential function (2). Sometimes, the number of exponentials exceeded three [57].

Table 1
Spectroscopy and photochemistry of hexahalide complexes of platinum group metals in aqueous and methanolic solutions. The spectral ranges explored in ultrafast experiments are indicated. LF stands for ligand-field bands, CT for charge–transfer and LMCT for ligand-to-metal charge-transfer bands.

Complex	Probe wavelength (nm)	Absorption band maxima (nm)	Transitions	Photochemical Properties vs. Solvent	
				H_2O	CH_3OH
$Ir^{IV}Cl_6^{2-}$	320	306	$d(t_{2g}) \rightarrow d(e_g{}^*)$ superimposed with LMCT $\pi(t_{1u}) \rightarrow d(t_{2g})$ [77]	Photoaquation $\phi_{aq} = 0.01$ [93]	Photoreduction $\phi_{red} = 0.1$ [94]
	405–420	415, 432	LMCT $\pi(t_{2u}) \rightarrow d(t_{2g})$ [77]	No reaction [93]	No reaction [94]
$Pt^{IV}Br_6^{2-}$	405–420	365 (strong) + 435 (weak)	$^1A_{1g} \rightarrow$ mixed (LF/CT) $^1T_{2g}$ [57]	Photoaquation $\phi_{aq} \sim 0.4$ [81,84]	Photoaquation + photoreduction $\phi_{aq} \approx 1.5\ \phi_{red}$ [10]
	530	525 (weak, LF)	LF $^1A_{1g} \rightarrow {}^3T_{1g}$ [57,78]	No information	
$Pt^{IV}Cl_6^{2-}$	405–420	362 (weak)	$d(t_{2g}) \rightarrow d(e_g{}^*)$ [76]	Photoaquation; ϕ_{aq} depends on excitation wavelength, intensity and $PtCl_6^{2-}$ concentration; chain processes [9]	Photoreduction [70,71]
$Ir^{IV}Br_6^{2-}$	770	745 (moderate)	LMCT $\pi(t_{2u}) \rightarrow d(t_{2g})$ [77]	No information	
$Os^{IV}Br_6^{2-}$	305	280 (strong)	LMCT $\pi \rightarrow d(e_g{}^*)$ [77]	No information	
	420	423 (moderate)	$\pi \rightarrow d(t_{2g})$ [77]		

$$\Delta A(\lambda,t)=A_1(\lambda)e^{-k_1t}+A_2(\lambda)e^{-k_2t} \tag{1}$$

$$\Delta A(\lambda,t)=A_1(\lambda)e^{-k_1t}+A_2(\lambda)e^{-k_2t}+A_3(\lambda)e^{-k_3t} \tag{2}$$

Provided that the kinetic curves may be satisfactorily fitted by the triexponential function (2), sequential decay of the transient absorption is assumed according to the scheme $A\rightarrow B\rightarrow C\rightarrow$ <ground state>. The species-associated difference spectra (SADS) of the individual components are then calculated using the expressions [59]:

$$S_A(\lambda)=A_1(\lambda)+A_2(\lambda)+A_3(\lambda) \tag{3}$$

$$S_B(\lambda)=A_2(\lambda)\frac{k_1-k_2}{k_1}+A_3(\lambda)\frac{k_1-k_3}{k_1} \tag{4}$$

$$S_C(\lambda)=A_3(\lambda)\frac{(k_1-k_3)(k_2-k_3)}{k_1k_2} \tag{5}$$

The formulas for SADS in biexponential decay (1), corresponding to the sequential decay of the transient absorption according to the reaction scheme $A\rightarrow B\rightarrow$ <ground state>, are

$$S_A(\lambda)=A_1(\lambda)+A_2(\lambda) \tag{6}$$

$$S_B(\lambda)=A_2(\lambda)\frac{k_1-k_2}{k_1} \tag{7}$$

In Expressions (3)–(7), A_i are the fitted transient amplitudes, S_X are the spectral absorbencies of the respective species, k_i are the reaction rate constants, and λ are the wavelengths.

Nanosecond laser flash photolysis experiments were performed using excitation by either a YAG laser (355 nm, 5 ns pulse duration, 5 mJ/pulse energy) or a XeCl excimer laser (XeCl laser, 308 nm, 15 ns, 10 mJ/pulse). The setup is described in [60]. Quantum yields were calculated based on measurements by a SOLO 2 laser power and energy metre (Gentec EO).

3. Results and discussion

3.1. Hexachloroplatinate

$Pt^{IV}Cl_6{}^{2-}$ is a $5d^6$ low spin octahedral complex. Its electronic absorption spectrum is shown in Fig. 1. The assignments of the absorption bands and the photochemical reactions caused by the excitation into these bands are listed in Table 1.

The $Pt^{IV}Cl_6{}^{2-}$ complex demonstrates redox photochemistry in aqueous solutions even without the addition of free Cl^- anions. Usually, homolysis of a Pt—Cl bond with a chlorine atom escaping from the solvent cage (8) is considered the primary photoreaction of $Pt^{IV}Cl_6{}^{2-}$ in aqueous solutions, as was first suggested in [61]. The same primary reactions were assumed in acetonitrile [62] and chloroform [63,64].

Nevertheless, the overall photochemical process is photoaquation, yielding the $Pt^{IV}Cl_5(H_2O)^-$ complex in the first stage [6,8,9,11,12,65,66]. Provided that atomic chlorine is produced in the primary Reaction (8), photoaquation may proceed via a chain reaction. Both the experimental data [6,8,9,11,12,65,66] and the quantum chemical calculations [66–68] show that $Pt^{III}Cl_{4-n}X_n$ ($n=1$–3; $X=OH^-$, H_2O) is the most probable chain carrier [6,11]. Depending on the experimental parameters (irradiation wavelength, light intensity, initial concentration of the complex, pH), the quantum yield may be either below unity [6,9,11] or significantly higher than unity [11,12]. The photoaquation chain reaction with the $Pt^{III}Cl_3(OH)^-$ complex as the chain carrier may be summarized as follows:

Table 2
The most intense absorption bands of the Pt(III) intermediates according to *X*α calculations by Goursot et al.

Complex	Geometry	Pt—Cl$_{ax}$ elongation (a.u.)	Intense absorption bands (nm)
$Pt^{III}Cl_6{}^{3-}$ [66]	Distorted O$_h$	0	175; 212
		0.2	207; 266
		0.4	235; 318
		1.0	330; 540
$Pt^{III}Cl_5{}^{2-}$	D$_{3h}$ [66]	0	264; 323; 329
	C$_{4V}$ [67]	0	206
		0.4	270
		1.0	448; 560
$Pt^{III}Cl_4{}^-$ [66]	Planar		410: 620
$Pt^{III}(Cl^-)_{6-m}(X)_m$,$X=OH^-$, H_2O; $m=0$–2 [8,68]	Distorted O$_h$		<300; 450
$Pt^{III}(Cl^-)_{4-n}(X)_n$, $X=OH^-$, H_2O, $n=1$–3 [8,68]	Planar		410–420nm

Chain initiation

$$Pt^{IV}Cl_6{}^{2-}\xrightarrow{h\nu}Pt^{III}Cl_5{}^{2-}+Cl^\bullet \tag{8}$$

$$Pt^{III}Cl_5{}^{2-}+2H_2O\rightarrow Pt^{III}Cl_4(OH)(H_2O)^{2-}+Cl^-+H^+ \tag{9}$$

$$Pt^{III}Cl_4(OH)(H_2O)^{2-}\rightarrow Pt^{III}Cl_3(OH)^-+H_2O+Cl^- \tag{10}$$

Chain propagation

$$\begin{aligned}&Pt^{III}Cl_3(OH)^-+Pt^{IV}Cl_6{}^{2-}+H_2O\\&\quad\rightarrow Pt^{IV}Cl_5(OH)^{2-}+Pt^{III}Cl_3(H_2O)+Cl^-\end{aligned} \tag{11}$$

$$Pt^{III}Cl_3(H_2O)\rightleftharpoons Pt^{III}Cl_3(OH)^-+H^+ \tag{12}$$

$$Pt^{IV}Cl_5(OH)^{2-}+H^+\rightleftharpoons Pt^{IV}Cl_5(H_2O)^- \tag{13}$$

Chain termination

$$\begin{aligned}2Pt^{III}Cl_3(OH)^-+2H_2O\rightarrow\ &Pt^{IV}Cl_4(OH)(H_2O)^-\\&+Pt^{II}Cl_2(OH)(H_2O)^-\end{aligned} \tag{14}$$

In addition to chain photoaquation, direct photoaquation may occur by back electron transfer in the {Pt(III) ion – Cl atom} geminate pair [10].

Electron transfer from an alcohol molecule to the excited complex [70–72] was reported as a primary photoreaction of $Pt^{IV}Cl_6{}^{2-}$ in alcoholic solutions following excitation at 308 nm. This reaction yields the $Pt^{III}Cl_6{}^{3-}$ intermediate complex and a hydroxyalkyl radical. The $Pt^{III}Cl_6{}^{3-}$ complex rapidly dissociates into $Pt^{III}Cl_5{}^{2-}$ and Cl^- [70]. In turn, the $Pt^{III}Cl_5{}^{2-}$ intermediate generates the relatively long-living $Pt^{III}Cl_4{}^-$ complex:

$$Pt^{IV}Cl_6^{2-}\overset{h\nu}{\rightleftharpoons}(Pt^{IV}Cl_6^{2-})* \tag{15}$$

$$(Pt^{IV}Cl_6^{2-})*\xrightarrow{CH_3OH}Pt^{III}Cl_6^{3-}+{}^\bullet CH_2OH+H^+ \tag{16}$$

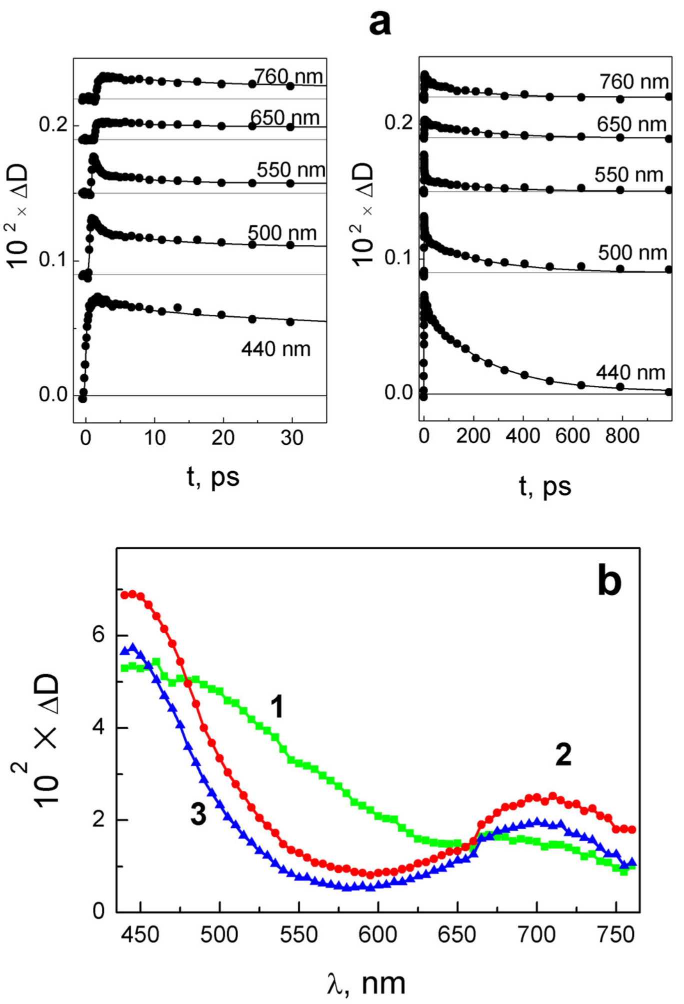

Fig. 2. Femtosecond photolysis of $Pt^{IV}Cl_6^{2-}$ (0.03 M) in aqueous solutions, $\lambda_{pump} = 405$ nm, 1 mm cuvette. (a) Kinetics of the transient absorption at different wavelengths and time ranges. Solid lines are the best three-exponential fits (Eq. (2)) after convolution with the instrument response function. (b) Species-associated difference spectra (SADS) of the consecutively formed intermediates (1 → 2 → 3). The best-fit characteristic times are 0.6, 8.6 and 220 ps.

$$Pt^{III}Cl_6^{3-} \rightarrow Pt^{III}Cl_5^{2-} + Cl^- \quad (17)$$

$$Pt^{\mathit{III}}C\ l_5^{2-} \rightarrow Pt^{III}Cl_4^- + Cl^- \quad (18)$$

$$Pt^{III}Cl_4{}^- + CH_3OH \rightarrow Pt^{II}Cl_4{}^{2-} + {}^{\bullet}CH_2OH + H^+ \quad (19)$$

This mechanism was supported by ESR detection of hydroxyalkyl radicals in frozen alcohols, both directly [73] and by spin trapping [74]. Specific intermediates identified as complexes of Pt (III) with free hydroxyalkyl radicals (radical complexes) were detected in the course of photolysis [71,72].

The first ultrafast spectroscopy study of $Pt^{IV}Cl_6{}^{2-}$ was presented by Goursot et al. [7]. They found that the excitation of $Pt^{IV}Cl_6{}^{2-}$ by 30 ps laser pulses at 355 nm resulted in the formation of an intermediate that had two absorption bands at 440 and 640 nm with a 210 ps lifetime. The intermediate was identified as either the $Pt^{III}Cl_5{}^{2-}$ (C_{4V}) complex or as an undetermined excited state of $Pt^{IV}Cl_6{}^{2-}$. This identification was based on the relativistic $X\alpha$ calculations of possible Pt(III) intermediates performed by Goursot et al. [7,66–68]; the results are collected in Table 2.

Recently, primary photochemical reactions in aqueous $Pt^{IV}Cl_6{}^{2-}$ were examined via femtosecond spectroscopy [10,69]. The excitation at 405 nm resulted in a transient absorption that decayed completely in 800 ps. Representative kinetic traces at several selected wavelengths are shown in Fig. 2a. The time profiles in the 440–780 nm wavelength range were fitted globally using a 3-exponential function (2) with lifetimes of $\tau_1 = 600$ fs, $\tau_2 = 8.6$ ps and $\tau_3 = 220$ ps. Fig. 2b demonstrates the SADS calculated using Eqs. (3)–(5). The synchronous behaviour of the two bands at approximately 450 and 700 nm justifies their attribution to the same intermediate, denoted Intermediate A. Intermediate A is most likely the same species as detected by Goursot et al. who could only probe up to 640 nm [7].

The properties and assignments of the Pt(III) intermediates according to [10] are collected in Table 3. In total, four intermediates were required to describe the experimental data. Note that Intermediate A was observed in the ultrafast experiments, while Intermediates C and D were observed in the microsecond time domain. Due to significantly different rates of Intermediate A decay and Intermediate C formation, an additional Intermediate B was introduced that is not directly observable in the visible spectral range. Among the different Pt(III) intermediates,

Table 3
Intermediates in the pulsed photolysis of $Pt^{IV}Cl_6{}^{2-}$ in H_2O. Note that λ_{max}, τ_{form} and τ_{dec} are the maximum of the absorption band and the intermediate formation and decay times [10].

Intermediate	λ_{max} (nm)	τ_{form}	τ_{dec}	Assignment
Aqueous solutions				
A	445, 700	600 fs	220 ps	$[Pt^{III}Cl_5{}^{2-}(C_{4v}) \ldots Cl^{\bullet}]$
B	–	<100 ns	1.2 μs	$Pt^{III}Cl_5{}^{2-}$ (D_{3h})
C	440–450	1.2 μs	7 μs	$Pt^{III}Cl_4X_2$ ($X = OH^-$, H_2O)
D	410	7 μs	>1 ms	$Pt^{III}Cl_{4-n}X_n$ ($n = 1$–3; $X = OH^-$, H_2O)
Methanolic solutions				
A	440, 700	700 fs	350 ps	$[Pt^{III}Cl_5{}^{2-}(C_{4v}) \ldots Cl^{\bullet}]$
E	no detectable absorption	<100 ns[b]	1 μs[b]	$Pt^{III}Cl_6{}^{3-}$
F	414	<50 ns[b,c]	2.6 ms[d]	$Pt^{III}Cl_5{}^{2-}$ (C_{4v})
	535	1.2 μs[b]		

[a] λ_{max}, τ_{form} and τ_{dec} are position of the absorption band maxima, formation and decay times of the intermediates.
[b] From [70].
[c] In a biphotonic process [70].
[d] From [75].

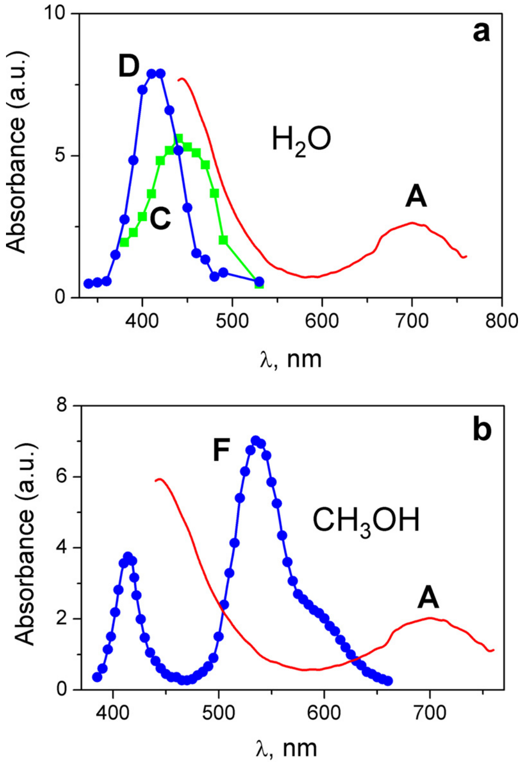

Fig. 3. Spectra of intermediates in the photolysis of $Pt^{IV}Cl_6{}^{2-}$ in water (a) and methanol (b). Intermediate A is the species detected in ultrafast experiments [10]. Intermediates C and D are the successive Pt(III) species detected in nanosecond laser flash photolysis experiments [9]. Intermediate F is a Pt(III) species detected in *X*eCl (308 nm, 15 ns) laser flash photolysis experiment (2 ms time delay) [70].

this lack of absorption is typical for $Pt^{III}Cl_6{}^{3-}$ and pentacoordinated $Pt^{III}Cl_5{}^{5-}$ complexes without sufficient distortions, while absorption in the visible spectral range is typical for complexes with close-to-planar structures (Table 2). The spectra of Intermediates A, C and D are shown in Fig. 3a.

Intermediate A was identified [10] as the Adamson's primary radical pair [4] with the structure $[Pt^{III}Cl_5{}^{2-}(C_{4v})\ldots Cl^\bullet]$, while the Intermediate B was identified as the $Pt^{III}Cl_5{}^{2-}$ complex with the trigonal bipyramidal (D_{3h}) structure. This identification is consistent with the calculations by Goursot et al. (Table 2). In contrast, identification of the Intermediate A as the $Pt^{III}Cl_5{}^{2-}$ (C_{4v}) complex instead of the radical pair, as proposed in [7], disagrees with the experiments on $Pt^{IV}Cl_6{}^{2-}$ photolysis in alcohols.

The primary reactions of aqueous $Pt^{IV}Cl_6{}^{2-}$ (Eqs. (20)–(25)) were proposed in [10,69]. Note that the formation of the $Pt^{III}Cl_5{}^{2-}$ (D_{3h}) complex is the starting point for the chain photoaquation of $Pt^{IV}Cl_6{}^{2-}$ (Eqs. (8)–(14)).

$$Pt^{IV}Cl_6^{2-}\xrightarrow{h\nu}[Pt^{IV}Cl_6^{2-}]*(^3T_{1g1g}) \quad (20)$$

$$[Pt^{IV}Cl_6^{2-}]*(^3T_{1g1g}) \rightarrow [Pt^{III}Cl_5^{2-}(C_{4V})\ldots Cl^\bullet] \quad (21)$$

Intermediate A (primary radical pair)

$$[Pt^{IV}Cl_6^{2-}]*(^3T_{1g1g}) \rightarrow Pt^{IV}Cl_6^{2-} \quad (22)$$

$$[Pt^{III}Cl_5^{2-}(C_{4V})\ldots Cl^\bullet] + H_2O \rightarrow [Pt^{III}Cl_5(H_2O)^{2-}\ldots Cl^\bullet] \quad (23)$$

Secondary radical pair

$$[Pt^{III}Cl_5(H_2O)^{2-}\ldots Cl^\bullet] \rightarrow Pt^{IV}Cl_5(H_2O)^{-} + Cl^{-} \quad (24)$$

$$[Pt^{III}Cl_5(H_2O)^{2-}Cl^\bullet] \rightarrow [Pt^{III}Cl_5^{2-}(D_{3h})] + Cl^\bullet H_2O \quad (25)$$

Intermediate B

Femtosecond laser excitation experiments on $Pt^{IV}Cl_6{}^{2-}$ in methanol and ethanol gave similar results to those obtained in aqueous solutions [10]. The results of the 3-exponential fit of the experimental kinetic curves in different solvents are collected in Table 4.

The fast formation of Intermediate A (600/700 fs) from the initial Franck–Condon state, which is a hot $^3T_{1g}$ state [76], was observed in both aqueous and alcoholic solutions of $Pt^{IV}Cl_6{}^{2-}$. The second and third reactions were identified [10] as the vibrational cooling of A and its return to the ground state $Pt^{IV}Cl_6{}^{2-}$ and/or transformation into long-lived photolysis products. The spectrum of Intermediate A in alcohols is the same as in aqueous solutions; therefore, it was identified as the $[Pt^{III}Cl_5{}^{2-}(C_{4v})\ldots Cl^\bullet]$ radical pair. The decay of Intermediate A is much faster than the formation of Intermediate F, observed on the microsecond time scale (Fig. 3b); therefore, the reaction mechanism A → E → F was postulated to include Intermediate E, with no detectable optical absorption in the near-UV or visible spectral ranges.

In alcohols, Intermediate A may oxidize a molecule of solvent present in the second coordination sphere of the complex anion, giving rise to the $Pt^{III}Cl_6{}^{3-}$ intermediate. The reaction mechanism based on the data from the nanosecond [70–72] and femtosecond [10] experiments is summarized by the Reactions ((20)–(22)) and ((26)–(31)), which use methanol as solvent.

$$[Pt^{III}Cl_5^{2-}(C_{4V})\ldots Cl^\bullet] + CH_3OH \rightarrow Pt^{III}Cl_6{}^{3-} + {}^\bullet CH_2OH + H^+ \quad (26)$$

Intermediate E

$$Pt^{III}Cl_6{}^{3-}\xrightarrow{h\nu,\ 308\ nm}(Pt^{III}Cl_6{}^{3-})* \quad (27)$$

$$(Pt^{III}Cl_6{}^{3-})* \rightarrow [Pt^{III}Cl_5^{2-}(C_{4V})] + Cl^{-} \quad (28)$$

Table 4
Characteristic lifetimes of the transient species after the excitation of the $Pt^{IV}Cl_6{}^{2-}$ complex into its visible *d*–*d* bands (405 nm) [10].

Solvent	τ_1 (ps)	Reaction	τ_2 (ps)	Reaction	τ_3 (ps)	Reaction
H_2O	0.6 ± 0.02	$^3T_{1g} \rightarrow A^*$	8.6 ± 4.5	$A^* \rightarrow A$	220 ± 30	Relaxation to the ground state + chemical reaction products
CH_3OH	0.7 ± 0.1		4.3 ± 1.1		350 ± 20	
C_2H_5OH	0.7 ± 0.2		11 ± 6		490 ± 50	

Intermediate F

$$\mathrm{Pt^{III}Cl_6}^{3-}\xrightarrow{t^\circ}[\mathrm{Pt^{III}Cl_5^{2-}}(C_{4V})]+\mathrm{Cl^-} \tag{29}$$

$$[\mathrm{Pt^{III}Cl_5^{2-}}(C_{4V})]\rightarrow[\mathrm{Pt^{III}Cl_4^{-}}]+\mathrm{Cl^-} \tag{30}$$

$$[\mathrm{Pt^{III}Cl_4^{-}}]+\mathrm{CH_3OH}\rightarrow[\mathrm{Pt^{II}Cl_4^{2-}}]+{}^\bullet\mathrm{CH_2OH}+\mathrm{H^+} \tag{31}$$

The $\mathrm{Pt^{III}Cl_6}^{3-}$ complex is distorted towards D_{4h} symmetry, with a moderate elongation of the axial Pt—Cl bonds; it exhibits LMCT transitions at approximately 308 nm [66] and does not absorb in the visible range. Therefore, Intermediate E was identified as $\mathrm{Pt^{III}Cl_6}^{3-}$. Its photochemical (Eqs. (27) and (28)) and thermal (Eq. (29)) reactions provide two pathways to the $\mathrm{Pt^{III}Cl_5}^{2-}$ complex (Intermediate F) [70,71]. According to the $X\alpha$ calculations [66], the C_{4v} structure of $\mathrm{Pt^{III}Cl_5}^{2-}$ with sufficient elongation of the axial Pt—Cl bond gives rise to the two-peak absorption spectrum in the visible spectral range. The intermediates identified in the $\mathrm{Pt^{IV}Cl_6}^{2-}$ photolysis in alcohols are collected in Table 3. The final product of $\mathrm{Pt^{IV}Cl_6}^{2-}$ photolysis in alcoholic solutions was identified as the $\mathrm{Pt^{II}Cl_4}^{2-}$ bivalent platinum complex [70–72,75]; prolonged irradiation of the latter gives rise to metallic platinum [13,14].

Finally, we identified the key intermediate observed in the femtosecond photolysis as the Adamson's primary radical pair $[\mathrm{Pt^{III}Cl_5}^{2-}(C_{4v})\ldots\mathrm{Cl}^\bullet]$. However, the precise nature of this intermediate is a question that is still open for discussion. One of the possibilities is to use ESR in low-temperature matrices to detect the presence of free radicals. Another feasible approach involves quantum chemical calculations of such radical complexes to determine their possible structures and properties.

3.3. Hexabromoplatinate

The $\mathrm{Pt^{IV}Br_6}^{2-}$ complex is isoelectronic to $\mathrm{Pt^{IV}Cl_6}^{2-}$. Its electronic absorption spectrum is shown in Fig. 1, with the assignments of the absorption bands and the photochemical reactions initiated by the respective excitations collected in Table 1. The most intense LMCT band of $\mathrm{Pt^{IV}Br_6}^{2-}$ is located at 226 nm. It corresponds to electron density transfer from σ-orbitals, which are predominantly located on ligands, to vacant σ*-orbitals, which are predominantly located on the metal ion [77]. The less intense charge transfer bands (290–450 nm), partially overlapping with the *d*–*d* bands, correspond to the transitions from the π-orbitals of the ligands [77]. The LMCT band with the maximum at 311 nm corresponds to the $\pi(t_{2u})\rightarrow d(e_g{}^*)$ and $\pi(t_{1u})\rightarrow d(e_g{}^*)$ transitions [57,77]. The absorption in the visible spectral range is caused by forbidden CT and mixed LF/CT transitions [57,58].

Earlier works on the photochemistry of $\mathrm{PtBr_6}^{2-}$ in aqueous solutions proposed contradictory reaction mechanisms. Adamson and Sporer [42] found that the quantum yield of the photoinduced ligand exchange in the $\mathrm{PtBr_6}^{2-}$—$\mathrm{Br^-}$ system significantly exceeds unity, postulating chain reactions to explain this fact. They assumed that the primary photolysis step was the homolytic cleavage of the Pt—Br bond with the formation of a Pt(III) intermediate and a bromine atom, similar to Reaction (8):

$$\mathrm{Pt^{IV}Br_6}^{2-}\xrightarrow{h\nu}\mathrm{Pt^{III}Br_5}^{2-}+\mathrm{Br}^\bullet \tag{32}$$

Nevertheless, Penkett and Adamson [79] in an experiment using lamp flash photolysis with a 30 μs time resolution failed to detect any transient absorption that could be attributed to the bromine atom, Pt(III) complexes, or products of their secondary reactions. They detected the aquated Pt(IV) complex as the final photolysis product on the sub-millisecond time scale, postulating the two-electron photoreduction of $\mathrm{Pt^{IV}Br_6}^{2-}$ with the escape of a $\mathrm{Br_2}$ molecule from the coordination sphere and the formation of the $\mathrm{Pt^{II}Br_4}^{2-}$ platinum(II) complex as the primary reaction:

$$\mathrm{Pt^{IV}Br_6}^{2-}\xrightarrow{h\nu}\mathrm{Pt^{II}Br_4}^{2-}+\mathrm{Br_2} \tag{33}$$

They stated that the $\mathrm{Pt^{II}Br_4}^{2-}$ complex is formed in the nonequilibrium (nonplanar) geometry, participating in the ligand exchange reaction as the chain carrier [79]. Thus, the step responsible for chain termination should be the backward redox reaction of the Pt(II) complex with $\mathrm{Br_2}$, restoring the Pt(IV) complexes. Thus, they explained the formation of the aquated Pt (IV) complex by the aquation of the $\mathrm{Pt^{II}Br_4}^{2-}$ complex, presenting no direct evidence of the chain photoaquation of $\mathrm{Pt^{IV}Br_6}^{2-}$ [79].

According to a different mechanism proposed by Balzani and co-workers [80–82], the cleavage of the Pt—Br bond is heterolytic and the $\mathrm{Pt^{IV}Br_5(H_2O)^-}$ aquated complex is the primary product of the photochemical reaction:

$$\mathrm{Pt^{IV}Br_6^{2-}}\underset{\mathrm{H_2O}}{\xrightarrow{h\nu}}\mathrm{Pt^{IV}Br_5(H_2O)^-}+\mathrm{Br^-} \tag{34}$$

Additionally, prolonged irradiation leads to further photoaquation of $\mathrm{Pt^{IV}Br_5(H_2O)^-}$ [63] with a quantum yield of the initial stage of approximately 0.4, which is independent of the irradiation wavelength [81].

Shagisultanova et al. [83] concluded that the experimental data on the $\mathrm{Pt^{IV}Br_6}^{2-}$ photolysis in strongly acidic solutions support the one-stage formation of the Pt(IV) complex with two water molecules in the first coordination sphere, thus proposing a trimolecular reaction that should have relatively low rates:

$$\mathrm{Pt^{IV}Br_6^{2-}}\underset{\mathrm{2H_2O}}{\xrightarrow{h\nu}}\mathrm{Pt^{IV}Br_4(H_2O)_2}+\mathrm{2Br^-} \tag{35}$$

Note that a recent study on the photochemistry of $\mathrm{Pt^{IV}Br_6}^{2-}$ in aqueous solutions [84] supports the hypothesis by Balzani et al. [80–82] on the multi-stage photoaquation of the complex. The authors re-examined the quantum yields of the first stage, obtaining the value of 0.39 in unbuffered aqueous solutions, 0.29 in pH 6.86 buffer, and 0.6 in 1 M $\mathrm{HClO_4}$ [84]. The nanosecond laser flash photolysis has only detected instant absorption changes occurring during the laser pulse; the spectrum of these changes coincides with the difference in the $\mathrm{Pt^{IV}Br_5(H_2O)^-}$ and $\mathrm{Pt^{IV}Br_6}^{2-}$ spectra [84]. Thus, the photoaquation reaction is faster than the 50 ns time resolution of the experimental setup [84].

Note that the addition of free bromide anions to aqueous solutions affected the $\mathrm{Pt^{IV}Br_6}^{2-}$ photolysis quite dramatically [85]. Indeed, nanosecond laser flash photolysis (308 nm) detected the formation of the $\mathrm{Br_2}^{\bullet-}$ radical anion, which reacted with the initial complex with the $k = 9\times10^8\ \mathrm{M^{-1}\,s^{-1}}$ rate constant, yielding a Pt(V) complex. The $\mathrm{Br_2}^{\bullet-}$ quantum yield data as a function of the bromide concentration demonstrate that the bromine atom is formed by electron transfer from a free $\mathrm{Br^-}$ anion to the photoexcited complex. Additionally, high concentrations of the bromide anion effectively suppress the competing photoaquation reaction.

There are only a few studies of the $\mathrm{Pt^{IV}Br_6}^{2-}$ photochemistry in organic solvents. Vasil'yev et al. [86] reported that its photolysis in acetonitrile results in photosolvation occurring via heterolytic cleavage of the Pt—Br bond:

$$\mathrm{Pt^{IV}Br_6^{2-}}\underset{\mathrm{CH_3CN}}{\xrightarrow{h\nu}}\mathrm{Pt^{IV}Br_5(CH_3CN)}+\mathrm{Br^-} \tag{36}$$

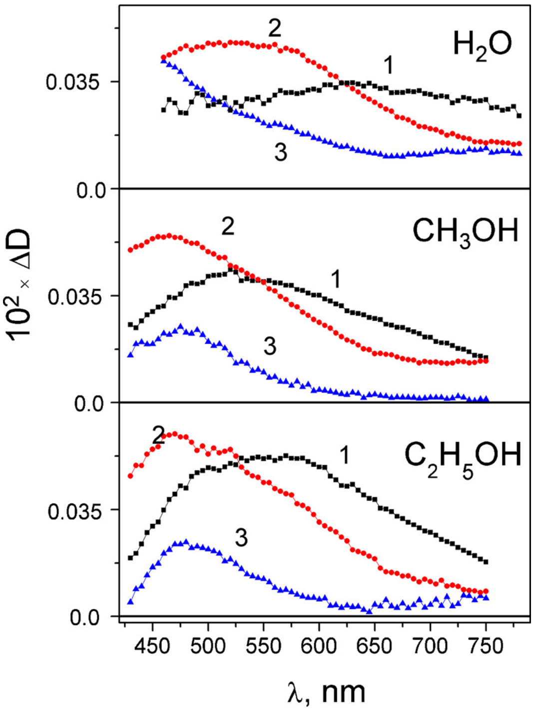

Fig. 4. Photolysis of $Pt^{IV}Br_6^{2-}$ in aqueous ($\lambda_{pump} = 420$ nm, 3.8×10^{-3} M), methanolic ($\lambda_{pump} = 405$ nm, 1.9×10^{-3} M) and ethanolic ($\lambda_{pump} = 405$ nm, 1.9×10^{-3} M) solutions. Curves 1–3 correspond to species-associated difference spectra (SADS) of the consecutively formed intermediates ($1 \to 2 \to 3$). The best-fit characteristic times are 0.4, 2.2 and 15 ps in water, 1.3, 8.7 and 130 ps in methanol, and 1.3, 9.6 and 260 ps in ethanol.

The photochemistry of $Pt^{IV}Br_6^{2-}$ in methanolic solutions was studied in [87], and the reaction products varied as a function of the dissolved oxygen. An outer-sphere electron transfer followed by the reduction of Pt(III) to Pt(II) was proposed in oxygen-free solutions:

$$PtBr_6{}^{2-} \xrightarrow[CH_3OH]{h\nu} PtBr_5{}^{2-} + {}^{\bullet}CH_2OH + H^+ + Br^- \tag{37}$$

$$PtBr_5{}^{2-} \rightarrow PtBr_4{}^{-} + Br^- \tag{38}$$

$$PtBr_4{}^{-} + \tilde{N}H_3OH \rightarrow PtBr_4{}^{2-} + {}^{\bullet}CH_2OH + H^+ \tag{39}$$

$$PtBr_6{}^{2-} + {}^{\bullet}CH_2OH \rightarrow H_2O + PtBr_5{}^{2-} + Br^- + H^+ \tag{40}$$

$$2{}^{\bullet}CH_2OH \rightarrow (CH_2OH)_2 \tag{41}$$

However, photosolvation of Pt(IV) with the formation of $Pt^{IV}Br_5(CH_3OH)^-$ occurred in the presence of dissolved oxygen. The effect of oxygen was explained by re-oxidation of the Pt(III) intermediates by the peroxide radicals [87]:

$${}^{\bullet}CH_2OH + O_2 \rightarrow {}^{\bullet}OOCH_2OH \tag{42}$$

$$PtBr_5{}^{2-} + {}^{\bullet}OOCH_2OH \rightarrow PtBr_5(CH_3OH)^- + O_2CH_2OH^- \tag{43}$$

Two types of intermediates were observed via lamp flash photolysis and interpreted as Pt(III) complexes, supporting the mechanisms outlined above [87]. Note that similar spectra of short-living Pt(III) bromide complexes were also obtained in pulse radiolysis experiments [88].

However, recently obtained results [10] are in apparent contradiction with the mechanisms proposed earlier [87]. Firstly, the removal of oxygen from methanolic solutions had no effect on the photolysis [10], in direct contradiction with previous results [87]. Secondly, nanosecond laser flash photolysis (308 nm) of $Pt^{IV}Br_6^{2-}$ in methanolic solutions detected no transient absorption kinetics; any reactions were faster than the 50 ns time resolution of the setup, resulting in instant absorption changes corresponding to the disappearance of the initial complex both in oxygen-free and in oxygen-saturated solutions. Continuous irradiation of $Pt^{IV}Br_6^{2-}$ at 313 nm resulted in photosolvation producing the $Pt^{IV}Br_5(CH_3OH)^-$ complex, with concurrent photoreduction producing the $Pt^{II}Br_4^{2-}$ complex [10]. The overall reactions could be described by Eqs. ((44)–(46)). However, in contrast to $Ir^{IV}Cl_6^{2-}$ (see below), no reaction of the ${}^{\bullet}CH_2OH$ radical with the initial complex could be detected [10]. The estimated ratio of the quantum yields of photosolvation and photoreduction at 313 nm was $\frac{\varphi_{solv}}{\varphi_{red}} \approx \frac{3}{2}$.

$$Pt^{IV}Br_6^{2-} \xrightarrow[CH_3OH]{h\nu} Pt^{IV}Br_5(CH_3OH)^- + Br^- \tag{44}$$

$$Pt^{IV}Br_6^{2-} \xrightarrow[CH_3OH]{h\nu} Pt^{III}Br_5^{2-} + {}^{\bullet}CH_2OH + Br^- + H^+ \tag{45}$$

$$Pt^{III}Br_5^{2-} + CH_3OH \rightarrow Pt^{II}Br_4^{2-} + {}^{\bullet}CH_2OH + Br^- + H^+ \tag{46}$$

Note that the photolysis of $Pt^{IV}Br_6^{2-}$ in frozen methanol (77 K) results in the reduction of Pt(IV) to $Pt^{II}Br_4^{2-}$, yielding the ${}^{\bullet}CH_2OH$ radical [89].

Ultrafast spectroscopy was also used to study the primary photophysical and photochemical reactions of $Pt^{IV}Br_6^{2-}$ in aqueous and alcoholic solutions [10,57,58,90]. The transient absorption spectra were fitted globally using the 3-exponential function (2) [10,90]. The SADS are shown in Fig. 4, and the characteristic reaction times and the respective reactions are listed in Table 5.

In [90], the fastest reaction was identified as the transition to the lower electronic excited state of $PtBr_6^{2-}$ (${}^3T_{1g}$), which is in agreement with the independence of quantum yield of photoaquation on the irradiation wavelength [81]. Nevertheless, according to [58], the lowest excited state of $PtBr_6^{2-}$ (${}^3T_{1g}$) dissociates spontaneously with a lifetime shorter than 150 fs. The

Table 5
Characteristic lifetimes of the transient absorption caused by excitation of the $Pt^{IV}Br_6^{2-}$ complex into its visible *d*–*d* bands (405 nm); 3-exponential fit (Eq. (2)).

Solvent	τ_1 (ps)	Reaction	τ_2 (ps)	Reaction	τ_3 (ps)	Reaction
H_2O	0.4	[a]$(PtBr_6{}^{2-})^* \rightarrow {}^3PtBr_5{}^- + Br^-$	2.2	${}^3PtBr_5{}^- \rightarrow {}^1PtBr_5{}^-$	15	${}^1PtBr_5{}^- \rightarrow PtBr_6{}^{2-}$ and $PtBr_5(H_2O)$
MeOH	1.3 ± 0.3	${}^3PtBr_5{}^- \rightarrow {}^1PtBr_5{}^-$ and [b] ${}^3PtBr_5{}^- + ROH \rightarrow {}^2PtBr_5{}^{2-}$	8.7 ± 1.4	${}^1PtBr_5{}^- + Br^- \rightarrow PtBr_6{}^{2-}$ and [b] ${}^1PtBr_5{}^- + ROH \rightarrow PtBr_5(ROH)$	130 ± 40	${}^2PtBr_5{}^{2-} + ROH \rightarrow PtBr_4{}^{2-}$ + products
EtOH	1.3 ± 0.5		9.6 ± 2.0		260 ± 80	

[a] $Pt^{IV}Br_6^{2-}$ (${}^1T_{1g}$, ${}^1T_{2g}$); the assignment of the absorption bands was provided by Zheldakov [57].
[b] $R = CH_3$; C_2H_5.

spectral changes were interpreted as the successive formation of the $\mathrm{Pt^{IV}Br_5}^-$ excited triplet and ground singlet states (Table 1, Eqs. (47)–(52)). Note that excitation of $\mathrm{Pt^{IV}Br_6}^{2-}$ at 420 nm and its direct excitation at 530 nm to the $^3T_{1g}$ state yield the same photoproducts.

Within 150 fs after the 420 nm excitation pulse, the $\mathrm{Pt^{IV}Br_6}^{2-}$ complex undergoes internal conversion and intersystem crossing into the $^3T_{1g}$ lowest triplet dissociative state, loses a ligand, and relaxes via the C_{4v} conical intersection to the nearly trigonal bipyramidal $^3\mathrm{Pt^{IV}Br_5}^-$ product in its triplet state [58]. The following reaction is the intersystem crossing of $^3\mathrm{Pt^{IV}Br_5}^-$ into its $^1\mathrm{PtBr_5}^-$ singlet state, the direct precursor of the $\mathrm{Pt^{IV}Br_5(H_2O)}^-$ complex, which is the reaction product. Thus, the transient absorption spectra 2 and 3 in Fig. 4, which were obtained in aqueous solutions, are attributed to the $^3\mathrm{Pt^{IV}Br_5}^-$ and $^1\mathrm{Pt^{IV}Br_5}^-$ species, respectively (see Table 5). Therefore, the $\mathrm{Pt^{IV}Br_6}^{2-}$ photolysis into its d–d bands may be described by the mechanism ((47)–(52)) [57,58], resulting in the experimentally observed quantum yield independence of the excitation wavelength.

$$\mathrm{Pt^{IV}Br_6^{2-}}(^1A_{1g1g})\xrightarrow{h\nu}\mathrm{Pt^{IV}Br_6^{2-}}(^1T_{1g1g}*,\ ^1T_{2g2g}*) \tag{47}$$

$$\mathrm{Pt^{IV}Br_6^{2-}}(^1T_{1g1g}*,\ ^1T_{2g2g}*) \rightarrow \mathrm{Pt}^{IV}\mathrm{B\ r_6^{2-}}(^3T_{1g1g}*) \tag{48}$$

$$\mathrm{Pt^{IV}Br_6^{2-}}(^3T_{1g1g}*) \rightarrow \{^3\mathrm{Pt^{IV}Br_5^-}\ldots\mathrm{Br^-}\}_{\mathrm{cage}} \tag{49}$$

$$\{^3\mathrm{Pt^{IV}Br_5^-}\ldots\mathrm{Br^-}\}_{\mathrm{cage}} \rightarrow \{^1\mathrm{Pt^{IV}Br_5^-}\ldots\mathrm{Br^-}\}_{\mathrm{cage}} \tag{50}$$

$$\{^1\mathrm{Pt^{IV}Br_5^-}\ldots\mathrm{Br^-}\}_{\mathrm{cage}} \rightarrow \mathrm{Pt^{IV}Br_6^{2-}}(^1A_{1g1g}) \tag{51}$$

$$\{^1\mathrm{Pt^{IV}Br_5^-}\ldots\mathrm{Br^-}\}_{\mathrm{cage}} + \mathrm{H_2O} \rightarrow \mathrm{Pt^{IV}Br_5(HO)^-} + \mathrm{Br^-} \tag{52}$$

The identification of the intermediates as the $^3\mathrm{Pt^{IV}Br_5}^-$ and $^1\mathrm{Pt^{IV}Br_5}^-$ species in [57,58] was supported via CASPT2 and DFT/TDDFT calculations of their absorption spectra and by observation of coherent oscillations in the early-time kinetic traces. Indeed, long-lived oscillations (with the oscillation decay time $\tau_{\mathrm{osc}} \sim 1.4$ ps) were recorded within the ground-state bleaching range and, therefore, assigned to the pulsed resonance Raman scattering from the ground state of $\mathrm{Pt^{IV}Br_6}^{2-}$. In contrast, the short-lived ($\tau_{\mathrm{osc}} < 400$ fs) oscillations reflect the vibrational modes of $^3\mathrm{Pt^{IV}Br_5}^-$. Thus, the $\mathrm{Pt^{IV}Br_6}^{2-}$ photolysis in aqueous solutions has been investigated along its entire pathway, starting from the absorption of a photon to the formation of the final reaction products.

Considering the $\mathrm{Pt^{IV}Br_6}^{2-}$ photolysis in alcoholic solutions [10,57], we need to interpret the formation of the relatively long-living (more than 100 ps) intermediate species (Fig. 4, Table 5). The mechanism includes the recombination of the $^1\mathrm{Pt^{IV}Br_5}^-$ complex with the $\mathrm{Br^-}$ anion in the solvent cage, within approximately 10 ps. It is solvated at similar reaction rates, giving the $\mathrm{Pt^{IV}Br_5(ROH)}^-$ complex (Reaction (53)), which is the final product. Spectrum 3 (Fig. 4, alcohols) thus corresponds to the Pt(III) intermediate – the $\mathrm{Pt^{III}Br_5}^{2-}$ complex, formed by electron transfer (54). Subsequently, the $\mathrm{Pt^{III}Br_5}^{2-}$ complex transfers a second electron from another solvent molecule, giving $\mathrm{Pt^{II}Br_4}^{2-}$, the final photoreduction product [10]. Thus, $\mathrm{Pt^{IV}Br_6}^{2-}$ photolysis in alcoholic solution involves parallel reactions of photosolvation and photoreduction. The respective mechanism may be described by Reactions ((47)–(52)), which are the same as in aqueous solutions. The additional Reactions ((53)–(55)) are presented here for methanol as the solvent. Note that the results of the ultrafast experiments are consistent with the data from the stationary and nanosecond experiments [10].

$$\{^1\mathrm{Pt^{IV}Br_5^-}\ldots\mathrm{Br^-}\}_{\mathrm{cage}} + \mathrm{H_3OH} \rightarrow \mathrm{Pt^{IV}Br_5(H_3OH)^-} + \mathrm{Br^-} \tag{53}$$

$$^3\mathrm{Pt^{IV}Br_5^-} + \mathrm{H_3OH} \rightarrow \mathrm{Pt^{III}Br_5^{2-}} + {}^\bullet\mathrm{H_2OH} + \mathrm{H^+} \tag{54}$$

$$\mathrm{Pt^{III}Br_5^{2-}} + \mathrm{H_3OH} \rightarrow \mathrm{Pt^{II}Br_4^{2-}} + {}^\bullet\mathrm{H_2OH} + \mathrm{H^+} + \mathrm{Br^-} \tag{55}$$

3.4. Differences in photochemistry of isoelectronic $\mathrm{Pt^{IV}Cl_6}^{2-}$ and $\mathrm{Pt^{IV}Br_6}^{2-}$ complexes

The dramatic differences in the photochemical properties of isoelectronic $\mathrm{Pt^{IV}Br_6}^{2-}$ and $\mathrm{Pt^{IV}Cl_6}^{2-}$ complexes have attracted interest for many years [2,3]. Based on the presented experimental data, these differences could be explained by two underlying fundamental causes.

First, different primary reactive intermediates are formed. Namely, the excited $\mathrm{Pt^{IV}Br_6}^{2-}$ promptly forms the $^3\mathrm{Pt^{IV}Br_5}^-$ active intermediate, which next gets solvated in only 15 ps. In contrast, in $\mathrm{Pt^{IV}Cl_6}^{2-}$ the initial Pt(III) intermediate identified as the Adamson radical pair is much more stable, which in aqueous solutions enables the escape of Pt(III) complexes from the solvent cage, resulting in chain photoaquation.

Another cause that was proposed earlier is a large difference in the reactivities of the bromide and chloride Pt(III) intermediates, which is the key factor in alcoholic solutions [3]. For bromide complexes, very fast electron transfer from the solvent molecules to Pt(III) is accompanied by a still faster Pt(IV) solvation, and all of the reactions are complete within 0.5 ns. For chloride complexes, the relative stability of the Pt(III) intermediates gives rise to several secondary reactions.

3.5. Hexachloroiridate

The electronic absorption spectrum of $\mathrm{Ir^{IV}Cl_6}^{2-}$ in aqueous solution is shown in Fig. 1, with the properties of the absorption bands listed in Table 1, along with information on the respective photochemistry.

$\mathrm{Ir^{IV}Cl_6}^{2-}$ is a $5d^5$ low-spin octahedral complex. Its UV spectrum (Fig. 1) contains strong absorption bands both in the visible and UV ranges. A simple assignment of the absorption bands using non-relativistic symmetry was performed by Jorgensen [77], who attributed the bands at 400–500 nm with the extinction coefficient of approximately 4000 $\mathrm{M^{-1}\,cm^{-1}}$ to LMCT transitions. He also assigned the relatively weak ($\varepsilon \sim 1000\ \mathrm{M^{-1}\,cm^{-1}}$) band at 306 nm to ligand-field transitions [77], most likely superimposed with more LMCT transitions. Later, Goursot et al. [91] assigned this band to LMCT transitions based on relativistic calculations, which was also supported by Case and Lopez [92].

The visible LMCT bands of $\mathrm{Ir^{IV}Cl_6}^{2-}$ are not photoactive either in aqueous (quantum yields below 10^{-4} [93]) or in alcoholic [94] solutions.

The UV photochemistry of $\mathrm{Ir^{IV}Cl_6}^{2-}$ in aqueous solutions with or without free chloride ions has been studied using stationary methods [93,95,96]. These papers present rather contradictory conclusions. Thus, one of the papers stated that the only photochemical process for $\mathrm{Ir^{IV}Cl_6}^{2-}$ is photoaquation, resulting in the formation of the $\mathrm{Ir^{IV}Cl_5(H_2O)}^-$ complex [95]. These ideas were criticized by Balzani et al. [93], who described competition between photoaquation and photoreduction of Ir(IV) to Ir(III). They have also demonstrated that the reaction pathways and quantum yields depend on the photolysis wavelength and the concentration of free chloride ions in aqueous solution. That is, excitation into the short-wave charge transfer band (254 nm) resulted in the formation of $Ir^{IV}Cl_5(H_2O)^-$ by photoaquation and $Ir^{III}Cl_5(H_2O)^{2-}$ by photoreduction, with the total quantum yield of 0.029, independent of the concentration of free Cl^- ions in solution. However, the relative contribution of photoreduction to the quantum yield increases linearly with the Cl^- concentration; this fact is properly accounted for by the proposed mechanism [93]. This mechanism is also in agreement with the Adamson model of radical pairs [4], including the successive formation of two intermediates, $[Ir^{III}Cl_5{}^{2-}...Cl^\bullet]$, the primary radical pair, and $[Ir^{III}Cl_5(H_2O)^{2-}...Cl^\bullet]$, the secondary radical pair. The latter then transforms into the final reaction products:

$$Ir^{IV}Cl_6^{2-} \xrightarrow[k_{-1}]{h\nu} [Ir^{III}Cl_5^{2-}...Cl^\bullet] \tag{56}$$

$$Ir^{IV}Cl_6^{2-} + H_2O \rightarrow [Ir^{III}Cl_5(H_2O)^{2-}...Cl^\bullet] \tag{57}$$

$$[Ir^{III}Cl_5(H_2O)^{2-}...Cl^\bullet] \rightarrow Ir^{IV}Cl_5(H_2O)^- + Cl^- \tag{58}$$

$$[Ir^{III}Cl_5(H_2O)^{2-}...Cl^\bullet] \rightarrow Ir^{III}Cl_5(H_2O)^{2-} + Cl^\bullet \tag{59}$$

$$[Ir^{III}Cl_5(H_2O)^{2-}...Cl^\bullet] + Cl^- \rightarrow Ir^{III}Cl_5(H_2O)^{2-} + Cl^\bullet{}_2^- \tag{60}$$

When aqueous $Ir^{IV}Cl_6{}^{2-}$ was irradiated in the near-UV at 313 nm, where LMCT and *d–d* bands are superimposed, only photoaquation with the 0.01 quantum yield was observed [93]. The same experiment in the presence of 1.2 M Cl^- produced photoreduced $Ir^{III}Cl_6{}^{3-}$ with 2×10^{-2} quantum yield. This new reaction path leading to photoreduction was not discussed in [93]; however, the electron transfer from a free outer-sphere Cl^- to the excited complex was later postulated to be the primary process [96]:

$$Ir^{IV}Cl_6^{2-} \xrightarrow{h\nu} (Ir^{IV}Cl_6^{2-})^* \xrightarrow{Cl^-} Ir^{III}Cl_6^{2-} + Cl^\bullet \tag{61}$$

Nanosecond laser flash photolysis (308 nm) was used in a photochemical study of aqueous $Ir^{IV}Cl_6{}^{2-}$ with or without added Cl^- [97]. In the absence of Cl^-, photoaquation of the excited complex yielding $Ir^{IV}Cl_5(H_2O)^-$ occurred within the 50 ns time resolution of the setup. Apparently, heterolytic cleavage of the Ir—Cl bond occurred (Reactions (62) and (63)) in the absence of any redox reactions:

$$Ir^{IV}Cl_6^{2-} \underset{k_{-1}}{\overset{h\nu}{\rightleftharpoons}} (Ir^{IV}Cl_6^{2-})* \tag{62}$$

$$(Ir^{IV}Cl_6^{2-})* \xrightarrow[k_2]{H_2O} Ir^{IV}Cl_5(H_2O)^- + Cl^- \tag{63}$$

However, the photoreduction of $Ir^{IV}Cl_6{}^{2-}$ and the formation of the $Cl_2{}^{\bullet -}$ radical anions occurred in the presence of free Cl^-, and the reaction quantum yield increased with the Cl^- concentration

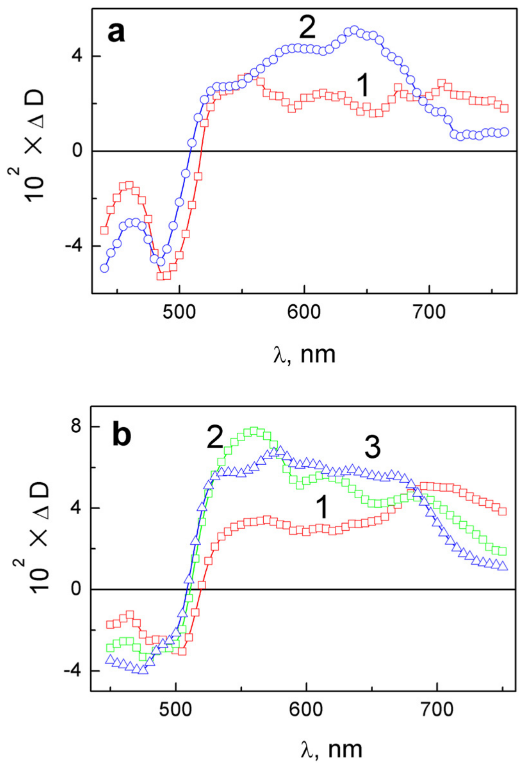

Fig. 5. Ultrafast photolysis of $Ir^{IV}Cl_6{}^{2-}$. 3×10^{-3} M initial concentration. (a) Photolysis in H2O, λ_{pump} = 420 nm; curves 1 and 2 correspond to species-associated difference spectra (SADS) of the consecutively formed intermediates (1 → 2). (b) Photolysis in methanol, λ_{pump} = 400 nm; curves 1–3 correspond to SADS of the consecutively formed intermediates (1 → 2 → 3). The best-fit characteristic times are 0.5 and 18 ps in water and 0.35, 2.2 and 30 ps in methanol.

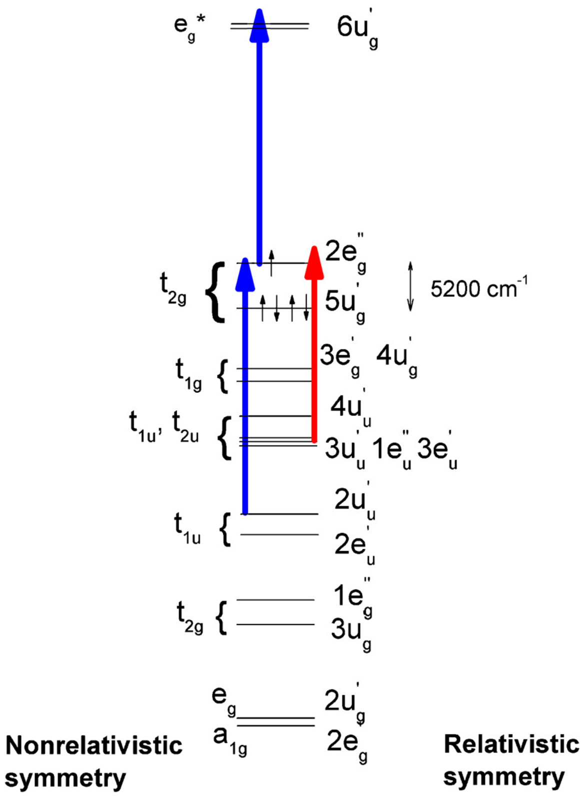

Fig. 6. The order of the molecular orbitals in the $Ir^{IV}Cl_6{}^{2-}$ complex according to [77]: non-relativistic approximation, left-hand side and [91]: relativistic approximation, right-hand side. Electrons in the filled orbitals below $5u_g{}'$ are omitted. The red arrow shows the 400 nm excitation, and the blue arrows show the 320 nm excitation.

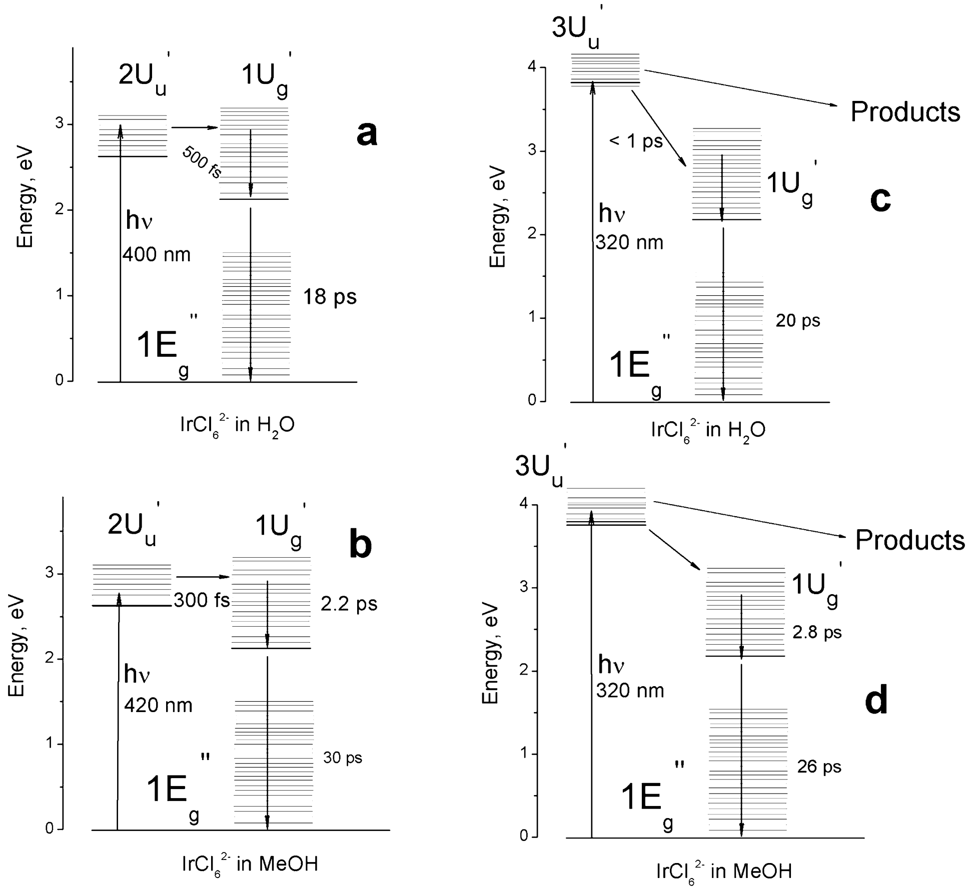

Fig. 7. Reactions subsequent to ultrafast excitation (a and b – at 400 nm; c and d – at 320 nm) of $Ir^{IV}Cl_6^{2-}$ in water (a and c) and methanol (b and d).

[97]. These results support the conclusion that a chlorine atom, which is a precursor of the $Cl_2^{\bullet -}$ radical ion, is produced by electron transfer from an outer-sphere Cl^- to the excited complex [96].

The photolysis of $Ir^{IV}Cl_6^{2-}$ in alcohols in the near-UV (313 nm) resulted in the photoreduction of Ir(IV) and the formation of the $Ir^{III}Cl_6^{3-}$ complex and a hydroxyalkyl radical [94,98]. Here, the primary reaction is the electron transfer from the solvent to the excited complex (Reaction (64)). The primary quantum yield of Ir (III) determined by Reactions (62) and (64) in simple alcohols is approximately 0.1 [98]; it is doubled in oxygen-free solutions due to Reaction (65) with the transient hydroxyalkyl radical [94]:

$$(Ir^{IV}Cl_6^{2-})* \overset{CH_3OH}{\rightarrow} Ir^{III}Cl_6^{3-} + {}^{\bullet}CH_2OH + H^+ \qquad (64)$$

$$Ir^{IV}Cl_6^{2-} + {}^{\bullet}CH_2OH \rightarrow Ir^{III}Cl_6^{3-} + CH_2O + H^+ \qquad (65)$$

Hydroxyalkyl radicals formed upon photolysis of $Ir^{IV}Cl_6^{2-}$ were observed directly in frozen methanol [99] and ethanol [100] matrices at 77 K. In the same conditions, weakly bound $[Ir^{III}Cl_6^{3-}...{}^{\bullet}CH_2OH]$ and $[Ir^{III}Cl_6^{3-}...CH_3{}^{\bullet}CHOH]$ radical complexes were stable at 77 K [99,100].

Similar to aqueous solutions, different mechanisms were proposed for the photochemistry of $Ir^{IV}Cl_6^{2-}$ in acetonitrile [101,102]. Indeed, Fukuzumi and Kochi [101] photolysed this complex at low temperatures, detecting the ESR spectrum of the chlorine atom at −170 °C, and concluding that inner-sphere charge transfer (56) was the primary reaction. In contrast, we were unable to detect any ESR signal even upon prolonged irradiation of $Ir^{IV}Cl_6^{2-}$ in frozen acetonitrile [102], observing step-by-step photosolvation at room temperature and the formation of $Ir^{IV}Cl_5(CH_3CN)^-$ in the first step [102], similar to what occurs in aqueous solutions.

Ultrafast pump–probe experiments were performed with the excitation of $Ir^{IV}Cl_6^{2-}$ into the low-energy LMCT bands at 400–420 nm to investigate the evolution of the respective excited states [103,104]. The transient absorption decayed completely in 100 ps, and typical SADS are shown in Fig. 5. The transient decays in aqueous solutions were adequately fitted by two exponentials (1) with $\tau_1 = 0.5$ ps and $\tau_2 = 18$ ps [103]. Here, the complete recovery of the ground state is consistent with the absence of the photochemical activity of these visible LMCT bands. The transient decays in alcohols were adequately described by three exponentials (2) with $\tau_1 = 350$ fs, $\tau_2 = 2.2$ ps and $\tau_3 = 30$ ps in methanol.

The approximate structure of the molecular orbitals of the $IrCl_6^{2-}$ complex is shown in Fig. 6. The left-hand numbering of the orbitals corresponds to the ligand-field theory applied to an octahedral $5d^5$ low spin complex [77], while the right-hand numbering corresponds to the relativistic approximation [91,92]; Griffith notations were used [105]. Note that e and u denote 2-dimensional and 4-dimensional irreducible representations of the O_h symmetry group generated by the spin–orbit coupling, similar to $j = 1/2$ and $j = 3/2$ in spherical symmetry. The red arrow marks the 400 nm excitation into the low-energy LMCT band, while the blue arrows mark the 320 nm excitation into the superposition of the *d*–*d* and LMCT bands. Within the non-relativistic description, excitation at 400–420 nm corresponds to the first Laporte-allowed $\pi(t_{2u}) \rightarrow d(t_{2g})$ LMCT band [77]. Due to the electron transfer, the hole moves from the lower 5d subshell to the filled $\pi(t_{2u})$ ligand molecular orbital, forming a vibrationally hot $(^2T_{2u})^*$ excited term. Within the more sophisticated description based on the relativistic approximation [91,92], $(2U_u')^*$ is the initially excited term. The $(2U_u')^*$ state then rapidly transforms into the $(1U_g')^*$ vibrationally hot lowest electronic excited state, which is formed by an electronic configuration with a hole in the $5u_g'$ orbital.

The photophysics of $Ir^{IV}Cl_6{}^{2-}$ excited into the visible LMCT bands is summarized in Fig. 7(a and b) [104]. The first characteristic time (500 fs) in aqueous solutions describes both the $3u_u' \rightarrow 5u_g'$ electronic transition and the vibrational relaxation. The first time in alcohols (approximately 300 fs) describes the electronic transition to the hot $1U_g'^*$ state. The second characteristic time (approximately 2.5 ps) describes the vibrational relaxation and the solvent diffusive relaxation, observed as the overall kinetics, as frequently occurs in the photophysics of coordination compounds, where for example, intersystem crossing and vibrational relaxation may have quite similar rates and be experimentally indistinguishable [43]. Thus, the relaxation in alcohols takes more time than in water, which is in line with larger solvent molecules and higher viscosities. Note that the final characteristic time (18–31 ps in different solvents) describes the transition from $1U_g'$ to the ground state.

Recently, the primary processes in aqueous and methanolic $Ir^{IV}Cl_6{}^{2-}$ were examined under excitation at 320 nm into the LMCT and *d*–*d* bands [106]. This could result in either $2u_u' \rightarrow 2e_g''$ or $2e_g'' \rightarrow 6u_g'$ electronic excitation (Fig. 6); for the first one, corresponding to the LMCT excitation, the hole in the $2u_u'$ orbital results in the $3U_u'$ excited state [91,92]. In contrast, the $2e_g'' \rightarrow 6u_g'$ transition corresponding to the *d*–*d* excitation forms the $t_{2g}{}^4e_g{}^1$ configuration, which has two quartet and eight doublet terms [91]. These ten terms split into twenty due to spin–orbit interaction. According to Goursot et al. [91], these twenty ligand-field states appear within the 250–500 nm interval, partly hidden under the more intense LMCT bands. Among these, four could be excited by 320 nm quanta: $2E_g''$, $7U_g'$, $3E_g'$, and $8U_g'$ [91].

The tentative schemes of the reactions caused by the absorbed photon are shown in Fig. 7(c and d) with only the $2u_u' \rightarrow 2e_g''$ transition shown for simplicity. Note that visible–light excitation causes no chemical change, while the reaction quantum yields for near-UV excitation in water and methanol are also rather low (0.01–0.1, see Table 1). The spectra and lifetimes of the SADS corresponding to the longer-lived intermediate ($1U_g'$ excited state) are quite similar in aqueous and alcoholic solutions. Therefore, any behaviour distinguishing the excitation at 320 nm from that at 400–420 nm occurs within the first 1–2 ps.

Thus, the excitation of $Ir^{IV}Cl_6{}^{2-}$ either into the visible LMCT bands or the mixed LMCT and *d*–*d* states in the near-UV region results in a transient absorption, decaying completely with the characteristic times of 20–30 ps. The observed ground state recovery is consistent with low photochemical activity of $IrCl_6{}^{2-}$ excited into the near-UV bands.

3.6. Hexabromoiridate

The $Ir^{IV}Br_6{}^{2-}$ complex is isoelectronic to the $Ir^{IV}Cl_6{}^{2-}$ $5d^5$ low spin octahedral complex. LMCT bands in its absorption spectrum were assigned by Jorgensen [77] to transitions from the ligand π-orbitals to the metal T_{2g} orbital at 500–900 nm or to the $E_g{}^*$ metal orbital at 250–450 nm. The photochemistry of $IrBr_6{}^{2-}$ has not been described, mainly because free Br^- is required to stabilize it in aqueous solutions. However, free halide anions in solution may cede electrons to the excited complex [96,107–109], adding complexity to the photolysis mechanism.

Rensing et al. [110] studied gas-phase $Ir^{IV}Br_6{}^{2-}$ using femtosecond photoelectron spectroscopy. Solutions of K_2IrBr_6 were electrosprayed, and the resulting gas phase $Ir^{IV}Br_6{}^{2-}$ was excited at 770 nm into the $\pi(t_{2u}) \rightarrow d(t_{2g})$ transition (see Table 1) using approximately 150 fs pulses. Several products were detected, i.e. $Ir^{IV}Br_5{}^-$, $Ir^{IV}Br_4$ and Br^-, indicating that $Ir^{IV}Br_6{}^{2-}$ dissociated from a hot ground state, formed by diabatic relaxation of the initial excited state. The latter was depopulated in a biphasic process with 2.1 and 21 ps characteristic lifetimes. The unimolecular dissociation occurred with an 80 ps characteristic time, which is determined by Br^- moving over the dissociation barrier.

To compare the photodynamics in the gas and liquid phases, Zheldakov [57] used ultrafast pump–probe spectroscopy with 770 nm excitation to photolyse aqueous $Ir^{IV}Br_6{}^{2-}$. He observed ground state bleaching at 484–618 and 654–736 nm, and new absorption appearing at 354–485 and 618–654 nm. The initially populated excited state decayed completely, with biexponential kinetics and 2.1 and 21 ps lifetimes, which are coincident with those obtained in the gas phase [110]. Zheldakov identified the formation and decay of the lowest electronic excited state of $Ir^{IV}Br_6{}^{2-}$ (Eq. (66); relativistic notation used for the terms, with the non-relativistic notation in brackets):

$$ {}^2E_{(T_{2g})} \overset{h\nu,\ 770\ \mathrm{nm}}{\longrightarrow} 2U'_g(T_{1g}) \overset{2\ \mathrm{ps}}{\longrightarrow} 2U'_g(T_{2g}) \overset{21\ \mathrm{ps}}{\longrightarrow} {}^2E_{(T_{2g})} \qquad (66) $$

Coherent oscillations with a 0.6-ps damping time, 110-fs induction period and 212 cm^{-1} frequency were observed in the excited state absorption. These oscillations were identified as the a_{1g} symmetric stretching of the Ir—Br bond, as confirmed by quantum-chemical calculations [57] and the experimental values of the Raman frequencies in $IrBr_6{}^{2-}$ [111].

Thus, no chemical reactions could be detected in aqueous $Ir^{IV}Br_6{}^{2-}$ solutions upon excitation at 770 nm, unlike the gas phase photodissociation of the complex [110]. This difference is explained by the fast dissipation of the vibrational energy in the condensed phase [57].

3.7. Hexabromoosmate

The electronic configuration of the $Os^{IV}Br_6{}^{2-}$ complex is $5d^4$ with the unequal occupation of the t_{2g} orbital set by the d^4 electrons distorting its geometry from O_h to D_{4h} symmetry [58].

The absorption spectrum of $Os^{IV}Br_6{}^{2-}$ was described by Jorgensen [77] and corresponds to transitions from the ${}^3T_{1g}$ triplet electronic ground state [57,112]. The LMCT bands from the ligand π-orbitals to the T_{2g} metal orbital at 380–620 nm, the *d*–*d* transitions at 350 nm and the LMCT from the ligand π-orbitals to the $E_g{}^*$ predominantly metal orbital at 280 and 245 nm were identified in the absorption spectrum [77,112]. Similarly to $Ir^{IV}Br_6{}^{2-}$, no photochemistry of $Os^{IV}Br_6{}^{2-}$ has been described.

The primary processes for $Os^{IV}Br_6{}^{2-}$ in aqueous and methanolic solutions were studied under 420 nm excitation (LMCT band, see Table 1) [57,58]. The transient absorption had a rather complex behaviour; the kinetics had to be fitted with five exponentials. The time constants in aqueous solutions, assuming a sequential reaction mechanism, were 70, 240, and 760 fs, 11.8 ps, and 1.2 ns [57]. The early-time (<100 fs) transient spectrum with absorption at 330–380 nm and 535–700 nm was assigned to the lowest triplet LF state. The two bands at 540 and 675 nm that form simultaneously between 100 fs and 1 ps and decay between 10 and 30 ps were attributed to the ${}^3Os^{IV}Br_5{}^-$ intermediate. The latter decayed producing an intermediate with three absorption bands with maxima at 365, 470 and 570 nm. This latter intermediate was identified as the $Os^{IV}Br_5(H_2O)$ aquated complex or its analogue in methanolic solutions. By the end of the time domain explored (1 ns) [57], the latter absorption decayed almost completely in methanolic solutions and very significantly in aqueous solutions. This latter fact had not been interpreted by the author [57].

Thus, Zheldakov [57] concluded that $Os^{IV}Br_6^{2-}$ photolysis is similar to that of $Pt^{IV}Br_6^{2-}$. The LMCT excitation at 420 nm leads to the triplet LMCT excited state, which is quickly depopulated by internal conversion to a lower-lying ^{3}LF state. This latter state is dissociative and decays with the formation of the $^3Os^{IV}Br_5^-$ triplet intermediate, which is a direct precursor of the solvated Os(IV) complexes, $Os^{IV}Br_5(H_2O)^-$or $Os^{IV}Br_5(CH_3OH)^-$, depending on the solvent.

The proposed reaction scheme was further supported by the observation of coherent oscillations and quantum-chemical calculations [57,58]. That is, oscillations that are characteristic for the $Os^{IV}Br_6^{2-}$ Raman spectra were observed at 208 cm^{-1} in the kinetic curves and correspond to the proposed $^3Os^{IV}Br_5^-$ intermediate. CASPT2 and DFT/TDDFT calculations of the triplet pentabromoosmate(IV) Raman frequencies supported this identification.

Therefore, the photochemical reaction mechanisms of $Os^{IV}Br_6^{2-}$ in aqueous and methanolic solutions based on fast photosolvation [57,58] explain almost all of the experimental results obtained in the ultrafast pump-probe experiments. Similarly, photosolvation was detected via stationary methods for the $Os^{IV}Cl_6^{2-}$ complex, which is isoelectronic with $Os^{IV}Br_6^{2-}$ [113]. The fact that was left unexplained in [57] is the disappearance of the proposed $Os^{IV}Br_5(H_2O)^-$ or $Os^{IV}Br_5(CH_3OH)^-$ complexes on the nanosecond time scale. New studies on the stationary and nanosecond laser flash photolysis of $Os^{IV}Br_6^{2-}$ are needed to complete the reaction mechanism for this complex.

4. Conclusions

For a complete description of photochemical reactions, we need to follow the entire reaction path from the ultrafast processes following excitation to the final products. Considering the five $M^{IV}X_6^{2-}$ complexes discussed here, the current state of knowledge is as follows:

- The information seems to be complete for the $Pt^{IV}Br_6^{2-}$ complex;
- The intermediates postulated for $Pt^{IV}Cl_6^{2-}$ photolysis should be verified against high-level quantum chemical calculations;
- The low quantum yields of $Ir^{IV}Cl_6^{2-}$ photolysis do not allow for correlation of the photophysical and photochemical experiments because there are no observable precursors of the stable photoproducts;
- Additional data on the stationary and nanosecond flash photolysis of $Os^{IV}Br_6^{2-}$ are required to complete its photolysis mechanism;
- The current state of knowledge for $Ir^{IV}Br_6^{2-}$ is the same as that for $Os^{IV}Br_6^{2-}$ with additional complications due to its instability in the absence of free Br^- anions.

Acknowledgements

Financial support from the Russian Foundation for Basic Research, Grant No. 14-03-00692, and Russian Scientific Foundation, Grant No. 15-13-10012, is gratefully acknowledged.

References

[1] J. Hershel, On the action of light in determining the precipitation of muriate of platinum by lime-water, Philos. Mag. 1 (1832) 58–60.
[2] V. Balzani, V. Carassiti, Photochemistry of Coordination Compounds, Acad. Press, New York, 1970 257–269, 307–312.
[3] P.C. Ford, J.D. Petersen, R.E. Hintze, Photochemistry of hexacoordinate complexes of the heavier transition metals, Coord. Chem. Rev. 14 (1974) 67–105.
[4] Concepts of Inorganic Photochemistry, in: A.W. Adamson, P.D. Fleischauer (Eds.), Wiley, New York, 1975, pp. 439.
[5] J. Sykora, J. Sima, Photochemistry of Coordination Compounds, Elsevier, 1990, 2015, pp. 225.
[6] R.C. Wright, G.S. Laurence, Production of platinum(III) by flash photolysis of $PtCl_6^{2-}$, J. Chem. Soc. Chem. Commun. (1972) 132–133.
[7] A. Goursot, A.D. Kirk, W.L. Waltz, G.B. Porter, D.K. Sharma, Experimental and theoretical study of the nascent photoredox behavior of the aqueous hexachloroplatinate(IV) ion, Inorg. Chem. 26 (1987) 14–18.
[8] W.L. Waltz, J. Lillie, A. Goursot, H. Chermette, Photolytic and radiolytic study of platinum(III) complex ions containing aquo and chloro ligands, Inorg. Chem. 28 (1989) 2247–2256.
[9] I.V. Znakovskaya, Yu.A. Sosedova, E.M. Glebov, V.P. Grivin, V.F. Plyusnin, Intermediates formed by laser flash photolysis of $PtCl_6^{2-}$ complex in aqueous solutions, Photochem. Photobiol. Sci. 4 (2005) 897–902.
[10] E.M. Glebov, A.V. Kolomeets, I.P. Pozdnyakov, V.F. Plyusnin, V.P. Grivin, N.V. Tkachenko, H. Lemmetyinen, Redox processes in photochemistry of Pt(IV) hexahaloid complexes, RSC Adv. 2 (2012) 5768–5778.
[11] L.E. Cox, D.G. Peters, E.L. Wehry, Photoaquation of hexachloroplatinate(IV), J. Inorg. Nucl. Chem. 14 (1972) 297–305.
[12] K.P. Balashev, V.V. Vasil'ev, A.M. Zimnyakov, G.A. Shagisultanova, Kinetics of chain reactions of photoaquation involving platinum(III) complexes, Koord. Khim. (Rus. J. Coord. Chem.) 10 (1984) 976–980.
[13] R.E. Cameron, A.B. Bocarsly, Photoactivated oxidation of alcohols by oxygen, J. Am. Chem. Soc. 107 (1985) 6116–6117.
[14] R.E. Cameron, A.B. Bocarsly, Multielectron-photoinduced reduction of chloroplatinum complexes: visible light deposition of platinum metal, Inorg. Chem. 25 (1986) 2910–2913.
[15] M. Sakamoto, M. Fujistuka, T. Majima, Light as a construction tool of metal nanoparticles: synthesis and mechanism, J. Photochem. Photobiol. C Photochem. Rev. 10 (2009) 33–56.
[16] N. Toshima, T. Takahashi, Colloidal dispersions of platinum and palladium clusters embedded in the micelles – preparation and application to the catalysis for hydrogenation of olefins, Bull. Chem. Soc. Jpn. 65 (1992) 400–409.
[17] N. Toshima, K. Nakata, H. Kitoh, Giant platinum clusters with organic ligands: preparation and catalysis, Inorg. Chim. Acta 265 (1997) 149–153.
[18] H. Einaga, M. Harada, Photochemical preparation of poly(*N*-vinyl-2-pyrrolidone)-stabilized platinum colloids and their deposition on titanium dioxide, Langmuir 21 (2005) 2578–2584.
[19] M. Harada, K. Okamoto, M. Terazima, Diffusion of platinum ions and platinum nanoparticles during photoreduction processes using the transient grating method, Langmuir 22 (2006) 9142–9149.
[20] M. Harada, H. Einaga, Formation mechanism of Pt particles by photoreduction of Pt ions in polymer solutions, Langmuir 22 (2006) 2371–2377.
[21] Yu. Borodko, P. Ercius, D. Zherebetskyy, Y. Wang, Y. Sun, G. Somorjai, From single atoms to nanocrystals: photoreduction of $[PtCl_6]^{2-}$ in aqueous and tetrahydrofuran solutions of PVP, J. Phys. Chem. C 117 (2013) 26667–26674.
[22] H. Chang, Y. Tsai, C. Cheng, C. Lin, P. Wu, Preparation of graphene-supported platinum nanoparticles in aqueous solution by femtosecond laser pulses for methanol oxidation, J. Power Sources 239 (2013) 164–168.
[23] L. Zang, W. Macyk, C. Lange, W.F. Mayer, C. Antonius, D. Meissner, H. Kish, Visible–light detoxification and charge generation by transition metal chloride modified titania, Chem. Eur. J. 6 (2000) 379–384.
[24] W. Macyk, H. Kish, Photosensitization of crystalline and amorphous titanium dioxide by platinum(IV) chloride surface complexes, Chem. Eur. J. 7 (2001) 1862–1867.
[25] X.Z. Li, F.B. Li, The enhancement of photodegradation efficiency using Pt–TiO_2 catalyst, Chemosphere 48 (2002) 1103–1111.
[26] H. Kish, Visible light photocatalysis by metal halide complexes containing titania as a semiconductor ligand, Adv. Inorg. Chem. 63 (Chapter 9) (2011) 371–393.
[27] F. Mahlamvana, R.J. Kriek, Photocatalytic reduction of platinum(II and IV) from their chloro complexes in a titanium dioxide suspension in the absence of an organic sacrificial reducing agent, Appl. Catal. B Environ. 148–149 (2014) 387–393.
[28] Q. Li, Zh. Chen, X. Zheng, Zh. Jin, study of photoreduction of $PtCl_6^{2-}$ on CdS, J. Phys. Chem. 96 (1992) 5959–5962.
[29] Zh. Jin, Q. Chen, Q. Li, Ch. Xi, X. Zheng, On the conditions and mechanism of PtO_2 formation in the photoinduced conversion of H_2PtCl_6, J. Photochem. Photobiol. A Chem. 81 (1994) 177–182.
[30] C. Harris, P.V. Kamat, Photocatalytic events of CdSe quantum dots in confined media. Electrodic behavior of coupled platinum nanoparticles, ACS Nano 4 (2010) 7321–7330.
[31] D. Lahiri, V. Subraminian, B.A. Bunker, P.V. Kamat, Probing photochemical transformations at TiO_2/Pt and TiO_2/Ir interfaces using X-ray absorption spectroscopy, J. Chem. Phys. 124 (2006) 1204720(1–7).
[32] P.J. Bednarski, F.S. Mackay, P.J. Sadler, Photoactivable platinum complexes, Anti-Cancer Agents Med. Chem. 7 (2007) 75–93.
[33] N. Cutillas, G.C. Yellol, C. de Haro, C. Vicente, V. Rodriguez, J. Riuz, Anticancer cyclometallated complexes of platinum group metals and gold, Coord. Chem. Rev. 257 (2013) 2784–2797.
[34] J. Pracharova, L. Zerzankova, J. Stepankova, O. Novakova, N.J. Farrer, P.J. Sadler, V. Brabec, J. Kasparkova, Interactions of DNA with a new platinum(IV) azide dipyridine complex activated by UVA and visible light: relationship to toxicity in tumor cells, Chem. Res. Toxicol. 25 (2012) 1099–1111.

[35] K.L. Swancutt, S.P. Mezyk, J.J. Kiddle, Free radical-induced redox chemistry of platinum-containing anti-cancer drugs, Radiat. Res. 168 (2007) 423–427.

[36] G.R. Gale, E.M. Walker Jr., A.B. Smith, A.E. Stone, Antitumor and antimutagenic properties of the photochemical reaction product of ammonium hexachloroiridate(IV), Proc. Soc. Exp. Biol. Med. 136 (1971) 1197–1202.

[37] J. Liu, P.J. Sadler, Organoiridium complexes: anticancer agents and catalysts, Acc. Chem. Res. (2014) , doi:http://dx.doi.org/10.1021/ar400266c Article ASAP.

[38] S. Moromizato, Y. Hisamatsu, T. Suzuki, Y. Matsuo, R. Abe, S. Aoki, Design and synthesis of a luminescent cyclometalated iridium(III) complex having *N*,*N*-diethylamino group that stains acidic intracellular organelles and induces cell death by photoirradiation, Inorg. Chem. 51 (2012) 12697–12706.

[39] S.P.-Y. Li, C.T.-Sh. Lau, H.-W. Louie, Y.-W. Lam, S.H. Cheng, K.K.-W. Lo, Mitochondria-targeting cyclometalated Ir(III)-PEG complexes with tunable photodynamic activity, Biomaterials 34 (2013) 7519–7532.

[40] A.K. Gupta, R.Z. Parker, R.J. Hanrahan, Solar-assisted production of hydrogen and chlorine from hydrochloric acid using hexachloroiridate(III) and (IV), Int. J. Hydrogen Energy 18 (1993) 713–718.

[41] A.K. Gupta, R.Z. Parker, C.E. Keefer, R.J. Hanrahan, Factors affecting quantum yields for chlorine formation in the solar photolysis of acidic chloride solutions containing hexachloroiridate(IV), Solar Energy 51 (1993) 409–414.

[42] A.W. Adamson, A.H. Sporer, Photochemistry of complex Ions. I. Some photochemical reactions of aqueous $PtBr_6^{2-}$, $Mo(CN)_8^{4-}$, and various Co(III) and Cr(III) complex Ions, J. Am. Chem. Soc. 80 (1958) 3865–3870.

[43] A. Vlcek Jr., The life and times of excited states of organometallic and coordination compounds, Coord. Chem. Rev. 200–202 (2000) 933–977 75.

[44] J.K. McCusker, Femtosecond absorption spectroscopy of transition metal charge–transfer complexes, Acc. Chem. Res. 36 (2003) 876–887.

[45] E.A. Juban, J.K. McCusker, Ultrafast dynamics of ^2E state formation in Cr $(acac)_3$, J. Am. Chem. Soc. 127 (2005) 6857–6865.

[46] L.S. Forster, Intersystem crossing in transition metal complexes, Coord. Chem. Rev. 250 (2006) 2023–2033.

[47] E.A. Juban, A.L. Smeigh, J.E. Monat, J.K. McCusker, Ultrafast dynamics of ligand-field excited states, Coord. Chem. Rev. 250 (2006) 1783–1791.

[48] J.N. Schrauben, K.L. Dillman, W.F. Beck, J.K. McCusker, Vibrational coherence in the excited state dynamics of $Cr(acac)_3$: probing the reaction coordinate for ultrafast intersystem crossing, Chem. Sci. 1 (2010) 405–410.

[49] S. Archer, J.A. Weinstein, Charge-separated excited states in platinum(II) chromophores: photophysics, formation, stabilization and utilization in solar energy conversion, Coord. Chem. Rev. 256 (2012) 2530–2561.

[50] A. Marino, P. Chakraborty, M. Servol, M. Lorenc, E. Collet, A. Hauser, The role of ligand-field states in the ultrafast photophysical cycle of the prototypical iron (II) spin–crossover compound $[Fe(ptz)_6](BF_4)_2$, Angew. Chem. Int. Edit. 53 (2014) 3863–3867.

[51] J.P. Lomont, S.C. Nguyen, C.B. Harris, Ultrafast infrared studies of the role of spin states in organometallic reaction dynamics, Acc. Chem. Res. 47 (2014) 1634–1642.

[52] R. Compton, H.K. Gerardi, D. Weidinger, D.J. Brown, W.J. Dressick, E.J. Heilweil, J.C. Owrutsky, Spectra and relaxation dynamics of the pseudohalide (PS) vibrational bands for $Ru(bpy)_2(PS)_2$ complexes, PS = CN, NCS and N_3, Chem. Phys. 422 (2013) 135–142.

[53] C. Sousa, C. de Graaf, A. Rudavskyi, R. Broer, J. Tatchen, M. Etinski, C.M. Marian, Ultrafast deactivation mechanism of the excited singlet in the light-induced spin crossover of $[Fe(2,2'\text{-bipyridine})_3]^{2+}$, Chem. Eur. J. 19 (2013) 17541–17551.

[54] N.V. Tkachenko, L. Rantala, A.Y. Tauber, J. Helaja, P.H. Hynninen, H. Lemmetyinen, Photoinduced electron transfer in phytochlorin-[60]Fullerene dyads, J. Am. Chem. Soc. 121 (1999) 9378–9387.

[55] S.V. Chekalin, The unique femtosecond spectroscopic complex as an instrument for ultrafast spectroscopy, femtochemistry and nanooptics, Phys. Usp. 49 (2006) 634–641.

[56] V. Voskresenska, R.M. Wilson, M. Panov, A.N. Tarnovsky, J.A. Krause, S. Vyas, A.H. Winter, C.M. Hadad, Photoaffinity labeling via nitrenium ion chemistry: protonation of the nitrene derived from 4-amino-3-nitrophenyl azide to afford reactive nitrenium ion pairs, J. Am. Chem. Soc. 131 (2009) 11535–11547.

[57] I.L. Zheldakov, Ultrafast photophysics and photochemistry of hexacoordinated bromides of Pt(IV), Os(IV), and Ir(IV) in the condensed phase studied by femtosecond pump–probe spectroscopy, Ph. D. Thesis, Bowling Green State University, 2010, 2015.

[58] I.L. Zheldakov, M.N. Ryazantsev, A.N. Tarnovsky, Wavepacket motion via a conical intersection in the photochemistry of aqueous transition-metal dianions, J. Phys. Chem. Lett. 2 (2011) 1540–1545.

[59] A.S. Rury, R.J. Sension, Broadband ultrafast transient absorption of iron(III) tetraphenyl porphyrine chloride in the condensed phase, Chem. Phys. 422 (2013) 220–228.

[60] I.P. Pozdnyakov, V.F. Plyusnin, V.P. Grivin, D.Yu. Vorobyev, N.M. Bazhin, E. Vauthey, Photochemistry of Fe(III) and sulfosalicylic acid aqueous solutions, J. Photochem. Photobiol. A Chem. 182 (2006) 75–81.

[61] R.L. Rich, H. Taube, Catalysis by Pt(III) of exchange reactions of $PtCl_4^{2-}$ and $PtCl_6^{2-}$, J. Am. Chem. Soc. 76 (1954) 2608–2611.

[62] K.P. Balashev, I.I. Blinov, G.A. Shagisultanova, Kinetics and mechanism for photosubstitution of the $[PtCl_6^{2-}]$ ion in acetonitrile, Kinet. Catal. 28 (1987) 696–700.

[63] O. Monreal, T. Esmaeli, P.E. Hoggard, A kinetic study of the photoreduction of hexachloroplatinate(IV) in chloroform, Inorg. Chim. Acta 265 (1997) 279–282.

[64] P.E. Hoggard, A. Vogler, The photooxidation of tetrachloroplatinate(II) in chloroform, Inorg. Chim. Acta 348 (2003) 229–232.

[65] K.P. Balashev, I.I. Blinov, G.A. Shagisultanova, Acidic-basic properties of platinum(III) chloride complexes, Zh. Neorg. Khim. (Russ. J. Inorg. Chem.) 32 (1987) 2470–2474 in Russian.

[66] A. Goursot, H. Chermette, E. Peigault, M. Chanon, W.L. Waltz, Xα method as a tool for structure elucidation of short-lived transients generated by pulse radiolysis or flash photolysis. I. Reductive reactions of $PtCl_6^{2-}$, Inorg. Chem. 23 (1984) 3618–3625.

[67] A. Goursot, H. Chermette, E. Peigault, M. Chanon, W.L. Waltz, Xα method as a tool for structure elucidation of short-lived transients generated by pulse radiolysis or flash photolysis. II. Oxidative reactions of $PtCl_4^{2-}$, Inorg. Chem. 24 (1985) 1042–1047.

[68] A. Goursot, H. Chermette, W.L. Waltz, J. Lillie, Theoretical study by the Xα method of platinum(III) complex containing aquo and chloro ligands, Inorg. Chem. 28 (1989) 2241–2247.

[69] E.M. Glebov, A.V. Kolomeets, I.P. Pozdnyakov, V.P. Grivin, V.F. Plyusnin, N.V. Tkachenko, H. Lemmetyinen, Chain processes in the photochemistry of Pt^{IV} halide complexes in aqueous solutions, Russ. Chem. Bull. 62 (2013) 1540–1548.

[70] V.P. Grivin, I.V. Khmelinski, V.F. Plyusnin, I.I. Blinov, K.P. Balashev, Photochemistry of $PtCl_6^{2-}$ complex in methanol solution, J. Photochem. Photobiol. A Chem. 51 (1990) 167–178.

[71] V.P. Grivin, I.V. Khmelinski, V.F. Plyusnin, Intermediates in the photoreduction of $PtCl_6^{2-}$ in methanol, J. Photochem. Photobiol. A Chem. 51 (1990) 379–389.

[72] V.P. Grivin, I.V. Khmelinski, V.F. Plyusnin, Primary photochemical processes of the $PtCl_6^{2-}$ complex in alcohols, J. Photochem. Photobiol. A Chem. 59 (1991) 153–161.

[73] G.A. Shagisultanova, Photochemical reactions of platinum(III) complexes studied by ESR method, Koord. Khim. (Russ. J. Coord. Chem.) 7 (1981) 1527–1531 in Russian.

[74] A.G. Fadnis, T.J. Kemp, Photo-oxidation of alcohols by hexachlorometalate(IV) ions (M = Pt, Pd, or Ir): spin trapping and matrix isolation electron spin resonance studies, J. Chem. Soc. Dalton Trans. (1989) 1237–1240.

[75] K.P. Balashev, I.I. Blinov, G.A. Shagisultanova, Kinetics and mechanism of photoinduced reactions of haloid complexes of platinum(III) in methyl alcohol, Koord. Khim. (Russ. J. Coord. Chem,) 12 (1987) 1674–1678 in Russian.

[76] A. Goursot, E. Penigault, H. Chermette, Relativistic MS Xα calculations of the electronic structure and related properties of $PtCl_6^{2-}$, Chem. Phys. Lett. 97 (1983) 215–220.

[77] C.K. Jorgensen, Electron transfer spectra of hexahalide complexes, Mol. Phys. 2 (1959) 309–332.

[78] C.K. Jorgensen, Complexes of 4d- and 5d-groups. II. Crystal field and electron transfer spectra of ruthenium(II) and (III), iridium(IV) and palladium(IV), Acta Chem. Scand. 10 (1959) 518–534.

[79] S.A. Penkett, A.W. Adamson, Flash photolysis of cobalt(III) acidopentaammine and of $PtBr_6^{2-}$ and PtI_6^{2-} complexes, J. Am. Chem. Soc. 87 (1965) 2514–2515.

[80] V. Balzani, V. Carassiti, F. Scandola, Electronic states in photochemistry of coordination compounds, Gazz. Chim. Ital. 96 (1966) 1213–1229.

[81] V. Balzani, M.F. Manfrin, L. Moggi, Photochemistry of coordination compounds. XVI. Hexabromoplatinate(IV) and hexaiodoplatinate(IV) ions, Inorg. Chem. 6 (1967) 354–358.

[82] V. Balzani, V. Carassiti, Photochemistry of some square-planar and octahedral platinum complexes, J. Phys. Chem. 72 (1968) 383–388.

[83] V.V. Vasil'ev, K.P. Balashev, G.A. Shagisultanova, Photosensitized reactions of hexabromoplatinate(IV) ion, Koord. Khim. (Russ. J. Coord. Chem.) 8 (1982) 1235–1240 in Russian.

[84] E.M. Glebov, V.F. Plyusnin, V.P. Grivin, A.B. Venediktov, S.V. Korenev, Photochemistry of $PtBr_6^{2-}$ in aqueous solutions, Russ. Chem. Bull. 56 (2007) 2357–2363.

[85] V.V. Vasil'ev, A.M. Zimnyakov, I.I. Blinov, Mechanism of photosubstitution reactions of $[Na_2PtBr_6]$ and *trans*-$[Pt(NH_3)_2Br_4]$ in acetonitrile, Koord. Khim. (Russ. J. Coord. Chem.) 13 (1987) 1528–11531 in Russian.

[86] K.P. Balashev, I.I. Blinov, G.A. Shagisultanova, Kinetics and mechanism of photoinduced reactions of halide complexes of Pt(III) in methyl alcohol, Koord. Khim. (Russ. J. Coord. Chem.) 13 (1987) 1674–1678 in Russian.

[87] R.K. Broszkiewicz, B. Voinovic, Redox reactions in aqueous solutions of $PtBr_4^{2-}$ and $PtBr_6^{2-}$, Radiat. Phys. Chem. 40 (1992) 11–16.

[88] E.M. Glebov, V.F. Plyusnin, A.B. Venediktov, S.V. Korenev, Photolysis of $[PtBr_6]^{2-}$ complex in the frozen methanol matrix, Russ. Chem. Bull. 52 (2003) 1305–1311.

[89] I.P. Pozdnyakov, E.M. Glebov, V.F. Plyusnin, N.V. Tkachenko, H. Lemmetyinen, Primary processes in photophysics and photochemistry of $PtBr_6^{2-}$ complex studied by femtosecond pump–probe spectroscopy, Chem. Phys. Lett. 442 (2007) 78–83.

[90] A. Goursot, H. Chermette, C. Daul, Relativistic calculation of the electronic structure and related properties of $IrCl_6^{2-}$, Inorg. Chem. 23 (1984) 305–314.

[91] J.P. Lopez, D.A. Case, Relativistic scattered wave calculations of hexachloro- and hexabromoiridate(IV), J. Chem. Phys. 81 (1984) 4554–4563.

[92] L. Moggi, G. Varani, M.F. Manfrin, V. Balzani, Photochemical reactions of hexachloroiridate(IV) ion, Inorg. Chim. Acta 4 (1970) 335–341.

[93] E.M. Glebov, V.F. Plyusnin, N.I. Sorokin, V.P. Grivin, A.B. Venediktov, H. Lemmetyinen, Photochemistry of $IrCl_6^{2-}$ complex in alcohols, J. Photochem. Photobiol. A Chem. 90 (1995) 31–37.

[94] T.P. Sleight, C.R. Hare, The photochemistry of hexachloroiridate(IV), Inorg. Nucl. Chem. Lett. 4 (1968) 165–167.

[95] P.K. Eidem, A.W. Mawerick, H.B. Gray, Production of hydrogen by irradiation of metal complexes in aqueous solutions, Inorg. Chim. Acta 50 (1981) 59–64.

[96] E.M. Glebov, V.F. Plyusnin, N.V. Tkachenko, H. Lemmetyinen, Laser flash photolysis of $IrCl_6^{2-}$ in aqueous solutions, Chem. Phys. 257 (2000) 79–89.

[97] E.M. Glebov, V.F. Plyusnin, V.P. Grivin, Yu.V. Ivanov, N.V. Tkachenko, H. Lemmetyinen, Photoreduction of $IrCl_6^{2-}$ complex in alcohol solutions and its reaction with hydroxyalkyl radicals, Int. J. Chem. Kinet. 30 (1998) 711–720.

[98] E.M. Glebov, V.F. Plyusnin, V.L. Vyazovkin, A.B. Venediktov, Photochemistry of the $IrCl_6^{2-}$ complex in methanol matrices, J. Photochem. Photobiol. A Chem. 107 (1997) 93–99.

[99] E.M. Glebov, V.F. Plyusnin, V.L. Vyazovkin, Photolysis of $IrCl_6^{2-}$ in frozen ethanol matrix, High Energy Chem. 33 (1999) 390–395.

[100] S. Fukuzumi, J.K. Kochi, Charge-transfer photochemistry in the cleavage of alkylmetals by hexachloroiridate(IV). ESR studies of paramagnetic intermediates, Inorg. Chem. 19 (1980) 3022–3026.

[101] E.M. Glebov, V.F. Plyusnin, Photochemistry of the $IrCl_6^{2-}$ complex in acetonitrile, Russ. J. Coord. Chem. 24 (1998) 507–511.

[102] A.V. Litke, I.P. Pozdnyakov, E.M. Glebov, V.F. Plyusnin, N.V. Tkachenko, H. Lemmetyinen, Photophysics of $IrCl_6^{2-}$ complex in aqueous solutions studied by femtosecond pump–probe spectroscopy, Chem. Phys. Lett. 477 (2009) 304–308.

[103] E.M. Glebov, A.V. Kolomeets, I.P. Pozdnyakov, V.F. Plyusnin, N.V. Tkachenko, H. Lemmetyinen, Ultrafast Pump-Probe Spectroscopy of $IrCl_6^{2-}$ complex in alcohol solutions, Photochem. Photobiol. Sci. 10 (2011) 1709–1714.

[104] J.S. Griffith, The Theory of Transition-Metal Ions, Cambridge University Press, Cambridge, UK, 1971.

[105] E.M. Glebov, I.P. Pozdnyakov, A.A. Melnikov, S.V. Chekalin, Photophysical and photochemical processes followed by 320 nm femtosecond laser excitation of $IrCl_6^{2-}$ complex in aqueous and methanol solutions, J. Photochem. Photobiol. A Chem. 292 (2014) 34–41.

[106] E.M. Glebov, V.F. Plyusnin, N.V. Tkachenko, H. Lemmetyinen, Photochemistry of the $IrCl_6^{2-}$ complex in aqueous solutions in the presence of the bromide anions, Russ. Chem. Bull. 57 (2008) 2487–2494.

[107] C. Rensing, O.T. Ehrler, J.-P. Yang, A.-N. Unterreiner, M.M. Kappes, Photodissociation dynamics of $IrBr_6^{2-}$ dianions by time-resolved photoelectron spectroscopy, J. Chem. Phys. 130 (2009) 234306(1–8).

[108] R.J.H. Clark, P.C. Turtle, Complex in aqueous solutions in the presence of the bromide anions effects. Resonance Raman spectroscopy of $[IrCl_6^{2-}]$, $[IrBr_6^{2-}]$, $[OsBr_6^{2-}]$ ions, J. Chem. Soc. Faraday Trans. 2 (74) (1978) 2063–2076.

[109] G.C. Allen, R. Al-Mobarak, G.A.M. El-Sharkawy, K.D. Warren, The electronic spectra of the hexahalo anions of osmium(IV) and iridium(IV), Inorg. Chem. 11 (1972) 787–796.

[110] E.M. Glebov, V.F. Plyusnin, V.P. Grivin, Yu.V. Ivanov, The photochemistry of the $OsCl_6^{2-}$ complex in water and methanol, Russ. J. Coord. Chem. 23 (1997) 580–585.